PHILOSOPHICAL TRANSACTIONS OF THE ROYAL SOCIETY B BIOLOGICAL SCIENCES

Demonstration of Cell Types among Cone Bipolar Neurons of Cat Retina

E. Cohen and P. Sterling

Phil. Trans. R. Soc. Lond. B 1990 **330**, 305-321
doi: 10.1098/rstb.1990.0201

Demonstration of cell types among cone bipolar neurons of cat retina

E. COHEN† AND P. STERLING

Department of Anatomy, University of Pennsylvania, Philadelphia, PA 19104, U.S.A.

SUMMARY

We identified all the cone bipolar cells (80) in a small patch of one retina and then studied in detail the complete subset (42) that sends axons to sublamina *b* of the inner plexiform layer. The point was to learn whether the 'types' suggested previously, based on a few examples from a large population, could be substantiated or whether there would be intermediate forms. Tissue from the area centralis (1° eccentricity), was prepared as a series of 279 ultrathin sections and photographed in the electron microscope. Thirteen cells were reconstructed completely and parcelled into five categories (b_1–b_5) based on external morphology. For nine of these cells (two from categories b_1–b_4 and one from b_5) most of the synaptic inputs and outputs were identified. When these nine cells were parcelled according to their synaptic patterns, they sorted into the same five categories. The remaining 29 cells in the population, though not reconstructed, were studied in detail by tracing their processes through the series. Ten of these cells, those near the margin of the series, were incomplete. The other 19 cells had essentially the same distribution of morphologies and synaptic patterns as the subset studied by total reconstruction: when plotted in multiparametric space, they formed distinct clusters corresponding to the five morphological categories. There was no hint of intermediate forms. That all the neurons in the population sort into some cluster (no intermediate forms), and that each neuron sorts into the same cluster by different criteria, argues that the clusters represent natural types. Each type forms a regular array in the region studied with an axonal 'coverage factor' that is close to one.

INTRODUCTION

This paper concerns the classification of cone bipolar cells in the cat retina based on their detailed structure and synaptic patterns. These neurons have been studied before and sorted into about 10 'types' (Boycott & Kolb 1973; Kolb *et al.* 1981; Famiglietti 1981; McGuire *et al.* 1984; Pourcho & Goebel 1987). However, here our concern is not primarily with the number of types but rather with how convincingly one can show that among cone bipolar neurons natural types truly exist.

The hypothesis that every retinal neuron belongs to a qualitatively distinct category ('type') has developed over roughly the last decade. Type refers to a unique set of features, including morphology, physiology, chemistry, and connections, that cluster in parametric space (Sterling 1982, 1983; Rodieck & Brening 1983). The hypothesis is potentially powerful because, if types are real, then to recognize them is to establish, in effect, a 'parts list' that can be used to study the functional architecture of retinal circuits (Sterling *et al.* 1988). The hypothesis is easy to accept where the number of categories is small and the distinctions between them are large, for example, the types A and B horizontal cells (Kolb 1974; Fisher & Boycott 1974; Boycott *et al.* 1978). However, where the number of categories is large, and the differences between them are subtle, a skeptic might assert that the categories lack objective reality and depend mainly on whether one is a 'splitter' or a 'lumper'.

This is the problem posed by the cone bipolar neurons. The cells in the area centralis are quite numerous, 38000 per square millimetre, 4–5 times the density of ganglion cells. The cone bipolar somas are roughly similar in size, shape, and cytology, and the processes, both dendritic and axonal, of most cone bipolar cells arborize narrowly. In short, the cells do not look very different, even to the experienced eye (figure 3). This forces the realization, emphasized by Rodieck, that what logically separates one category from another is nothing in particular about their respective 'looks' but rather the absence of intermediate forms (Rodieck & Brening 1983; Rodieck 1989). If intermediate forms exist, then categories can only be defined arbitrarily, and the idea that there are natural categories is not compelling.

Previous studies of cone bipolar neurons, most of which used the Golgi method, do not address this issue. On the contrary, although they show neurons that differ in morphology, the examples are not drawn from the same animal nor from the same retinal locus. Consequently, one cannot evaluate whether the differences define cell types or merely reflect variation between animals and/or different retinal loci. Neither can one be certain that quantitation of the differences

† Present address: Department of Physiology, University of Minnesota, MN 55455, U.S.A.

Phil. Trans. R. Soc. Lond. B (1990) **330**, 305–321
Printed in Great Britain
Vol. 330. B 1258 21 [Published 29 December 1990

would substantiate the hypothesis of types by documenting the absence of intermediate forms. Finally, one must always wonder with the Golgi method whether intermediate forms may actually exist but fail to impregnate.

To control for differences in eccentricity and differences between animals, an earlier study from our laboratory reconstructed bipolar cells from a small region of one retina (McGuire *et al.* 1984). However, only 15 cells were examined in detail, so for many categories there was only one example. Thus the possibility remained that what seemed to be discrete categories really belong to a continuum.

In the present study we identified all the cone bipolar cells in a small patch of one retina. The point was to see if we could substantiate the categories suggested previously or if there would be intermediate forms. This tissue had been prepared as a series of ultrathin sections and photographed in the electron microscope. Earlier work (Cohen & Sterling 1986) had shown it to contain the axons of 80 cone bipolar neurons partitioned equally between the outer one third of the inner plexiform layer (sublamina *a*) and the inner two thirds (sublamina *b*). (This approach to dividing the inner plexiform layer originates with Famiglietti & Kolb (1976); see also figure 6 in McGuire *et al.* (1984)). Since the task now was to study every cell in a population, we restricted our efforts to the subset of bipolar neurons innervating sublamina *b*.

METHODS

The tissue was taken from an adult cat that had been deeply anaesthetized with pentobarbital (40 mg/kg^{-1}), injected intraocularly with [^{3}H]glycine, and perfused an hour later with a phosphate-buffered mixture of 2% (w/w) glutaraldehyde and 2% (w/w) paraformaldehyde. The retina was postfixed in osmium tetroxide, stained with uranyl acetate, dehydrated and embedded in Epon. Tissue was cut vertically as a series of 279 ultrathin sections (approximately 0.09 μm thick). These were prepared as autoradiograms and then photographed at ×2200 in an electron microscope. (The patterns of [^{3}H]glycine accumulation in bipolar neurons have been described elsewhere (Cohen & Sterling 1986) and are not considered further here). Neurons were reconstructed by tracing their profiles in successive sections onto acetate sheets aligned on a cartoonist's jig. These tracings were then digitized and 'stacked' by a personal computer and printed in radial or tangential view with the hidden lines removed. For additional technical detail consult Stevens *et al.* (1980); Smith (1987); Cohen & Sterling (1986).

RESULTS

(*a*) *Nomenclature*

Since one point of this paper is that 'type' is an attribute to be shown, the results section refers to cell groupings as 'categories', deferring until the discussion the issue of whether a category constitutes a natural type. In naming a category we follow the system of McGuire *et al.* (1984), which first lists the sublamina (*a* or *b*) in which an axon terminates and then lists a numeral (subscripted by McGuire *et al.* (1984), but not Pourcho & Goebel (1987) who also adopted this approach). Since the only cells considered here are *c*one *b*ipolars, we omit, as redundant, the prefix 'CB'.

It is natural to wonder whether the categories we call b_1, b_2, etc. match categories called CBb_1, etc. by McGuire *et al.* and CBb1, etc. by Pourcho & Goebel. The answer in certain cases is 'yes' and in others 'no' or 'not exactly'. Readers exasperated at this news and wanting an immediate explanation, should recall that our present goal is to show a classification in a small patch of one retina. Only when this is accomplished are comparisons possible to different retinas, different eccentricities, and different methods. Therefore, we defer such comparisons to the discussion.

(*b*) *Location in retina*

The patch of retina studied was 25 × 90 μm and located on the horizontal meridian in the area centralis just nasal to the centre (figure 1, upper). Here the ganglion cell layer is a continuous tier 1–2 cells deep and contains no blood vessels (figure 1*c*). The patch was eccentric by about 1° as judged by the density of cones (24 200 mm^{-2}) (Steinberg *et al.* 1973) and cells in the ganglion cell layer (11 600 mm^{-2}). In these respects it resembled the retinal patch used in previous studies from this laboratory (McGuire *et al.* 1984, 1986; Freed & Sterling 1988; Sterling *et al.* 1988).

(*c*) *Neurons studied*

In this patch of central retina sublamina *b* contained the arborizations of 42 cone bipolar axons. Thirty four of these were traced from somas in the inner nuclear layer (figure 2); eight axons, being close to one edge or another of the patch, could not be traced to somas. We reconstructed 13 out of the 34 bipolar cells (38%). Based on certain morphological differences (to be discussed) we sorted the 13 cells into five categories. Then we studied the remaining 29 cells (in detail but without graphic reconstruction) to learn whether they fit easily into the established morphological categories or were intermediate. Finally, we reconstructed fully the synaptic patterns for two cells in each morphological category (except for category b_5 which had only one member) and then studied the synaptic patterns on the remaining 29 cells. Our purpose was to see whether sorting the cells by their synaptic patterns would give the same result as sorting them by morphology.

(*d*) *Morphology*

Figure 3 shows a vertical view of five cone bipolar neurons reconstructed from the retinal patch. These cells were separated in the tangential plane by no more than about 20 μm. The somas seem roughly similar: in diameter, depth in the inner nuclear layer, and cytology (figure 4). The dendritic and axonal arbors seem roughly similar in lateral extent and laminar

PHILOSOPHICAL TRANSACTIONS OF THE ROYAL SOCIETY B BIOLOGICAL SCIENCES

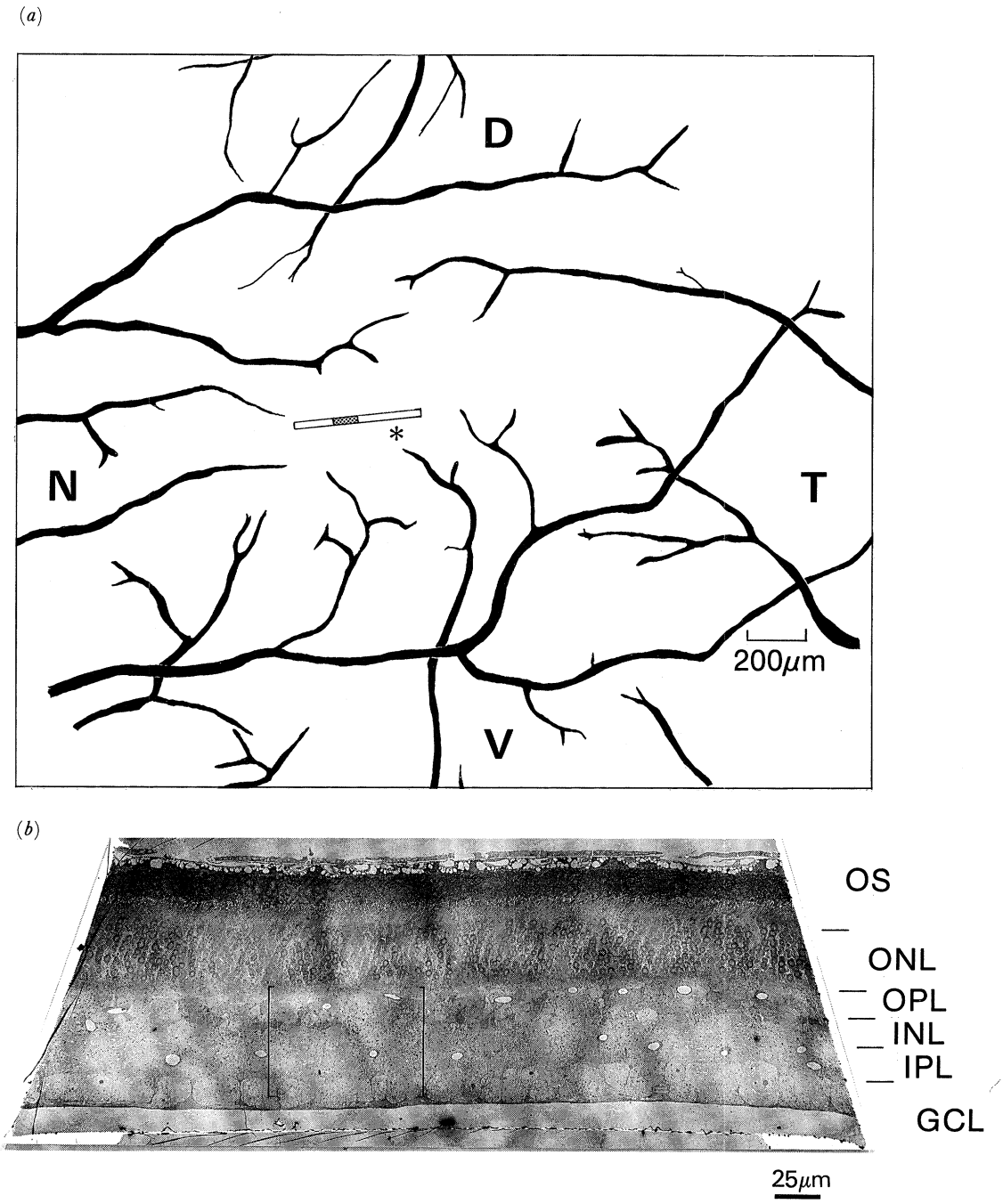

Figure 1. (*a*) Drawing of the area centralis in retinal wholemount. Converging dark lines represent blood vessels on the retinal surface which are seen to avoid the area centralis. Rectangle shows location and extent of tissue used for thin sections; hatched area shows region photographed in the electron microscope. The star marks centre of area centralis as estimated from the peak of ganglion cell density in the wholemount. N, nasal; T, temporal; D, dorsal; V, ventral. (*b*) Electron micrograph (low magnification) of section 274. Brackets show the region analysed. Neurons in the ganglion cell layer (GCL) form a continuous tier at this location, and blood vessels are absent. OS, outer segments; ONL, outer nuclear layer; OPL, outer plexiform layer; INL, inner nuclear layer; IPL, inner plexiform layer.

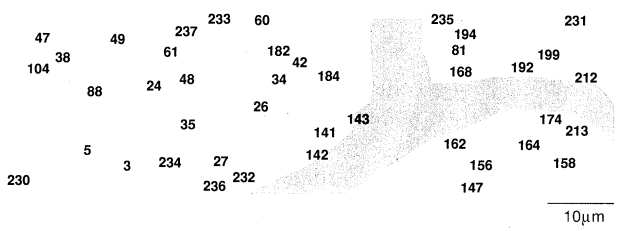

Figure 2. Location in tangential plane of all 42 cone bipolar axons that arborize in sublamina *b*. Distribution density, 19250 per square millimetre; nearest neighbour distance, 3.9 ± 4.4 μm. Shaded area indicates blood vessel at the junction of sublaminae *a* and *b*.

distribution. Some differences may be noted: the soma labelled b_3 is deepest, and its ascending and descending processes are the thinnest; the dendritic field of the cell labelled b_5 is the widest; the axon arborization of the cell labelled b_4 is the flattest in the tangential plane; the b_3 and b_4 axons are the shallowest, and the b_1 axon is the deepest. Whether these differences define categories obviously depends on the properties of the rest of the bipolar cells in the patch.

Figure 5 shows three members of the b_1 category. These neurons were located no further apart from each other in the tangential plane than 50 μm, and they

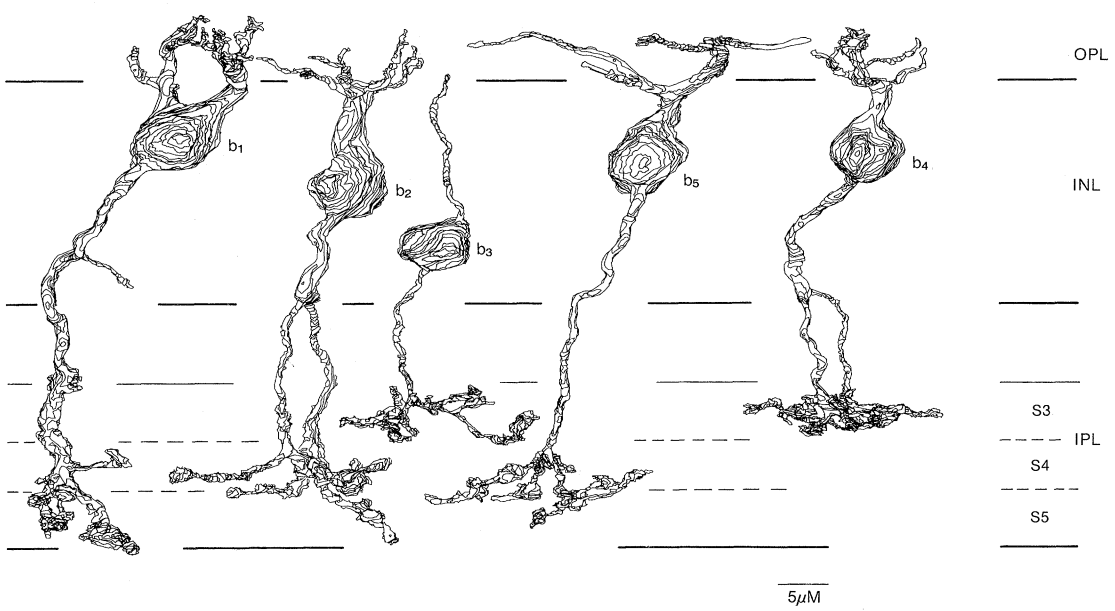

Figure 3. Vertical view of five cone bipolar neurons (one example from each category) reconstructed from electron micrographs of serial sections. Note that the axonal arbors are all limited to sublamina *b* and are narrow-field. The dendritic arbors of b_1, b_2, and b_4 are also narrow-field, and so probably is that of b_3, but it could not be traced.

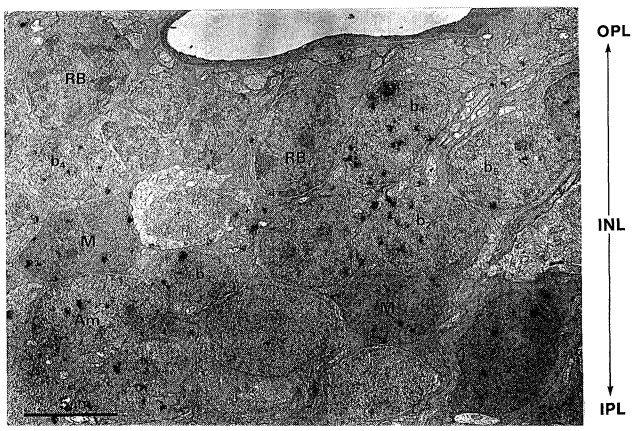

Figure 4. Electron micrograph of the inner nuclear layer (INL) (vertical view). Somas of different cone bipolar categories are roughly similar in size and cytological appearance, but occupy different levels in the INL (see figure 3). RB, rod bipolar; M, Muller cell; Am, amacrine cell.

seem similar in many respects. The somas are all high in the inner nuclear layer (INL) and the dendrites sprout from their upper surfaces like stalks from a carrot. The dendrites are rather stubby and the arbors are seen in tangential view to lack radial symmetry. The axons have claw-like arbors with chemical synaptic inputs (open circles) and outputs (dots) in all three strata of sublamina *b*. The outputs are seen in tangential view to concentrate about the axis of stalks rather than at the distal axon branches.

Figure 6 shows three members of the b_2 category. These neurons were separated in the tangential plane by no more than 50 μm. The somas are all at the middle of the INL, and the dendrites emerge in a gradual taper. The dendrites are relatively long and slender, and the arbors in tangential view exhibit varying degrees of radial symmetry (cf. cells 47 and 174). The axonal processes are somewhat thick and the arbors are flattened. Most of their synaptic inputs and outputs are in stratum 4 of sublamina *b*, with a modest number in stratum 5, and hardly any in stratum 3. The outputs are seen in the tangential view for one cell (no. 47) to distribute rather evenly along the axon branches and for the other cell (no. 26) to be more concentrated near the central stalk.

Figure 7 shows three members of the b_3 category. These neurons were separated in the tangential plane by no more than 40 μm. The somas are relatively small and deep in the INL. From each soma there emerges abruptly a single thin dendritic stalk. This ascends without branching to the outer plexiform layer (OPL) where it becomes too fine to trace. The axonal processes are also relatively thin, and the arbors are quite flattened. Almost all the inputs and outputs are in stratum 3, and they are seen in tangential view to distribute fairly evenly along the branches.

Figure 8 shows three members of the b_4 category. The neurons are separated in the tangential plane by no more than 35 μm. The somas are slightly higher in the INL than the b_2 cells and slightly lower than the b_1 cells. The dendrites emerge in a gradual taper, resembling somewhat the forms of b_2 but differing markedly from those of b_3. The dendrites of b_4 are relatively slender and the arbor may be either radially symmetrical about the dendritic stalk or highly asymmetrical (cf. cells 24 and 184, figure 8). The descending axonal process is noticeably thicker than that of b_3. The axonal arbor is somewhat broader than that of b_3, but it is similarly flattened and occupies the same stratum (S3) in sublamina *b*. The synaptic outputs are seen in tangential view to distribute extremely evenly along the axonal branches.

Figure 9 shows the only member of the b_5 category present in the retinal patch; it is located near the centre. The soma is at the same level in the INL as the b_4 cells, and the dendrites emerge, as for b_4, in a gradual taper. However, the soma is markedly larger

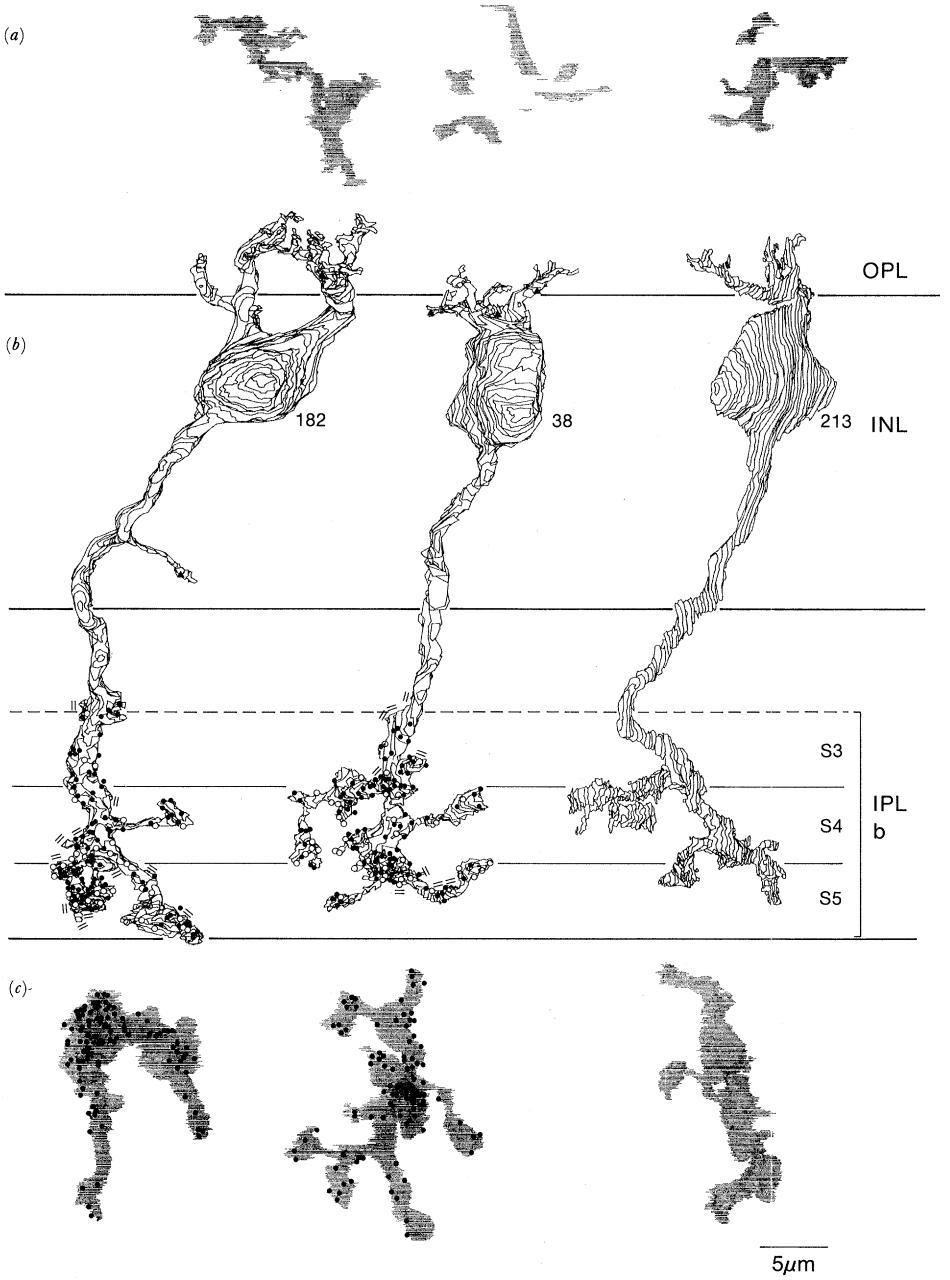

Figure 5. (*a*) Dendritic arbor of each cell in tangential view. (*b*) Reconstructions in vertical view of three b_1 bipolar neurons. Numbers next to soma are for identification. Dots, sites of chemical synaptic output; open circles, sites of chemical synaptic input; triangles, chemical synaptic contacts presumed to be from interplexiform cell; double bars, sites of gap junction with AII amacrine cells; single bars, sites of gap junction with cone bipolar cell. (*c*) Axonal arbor of each cell in tangential view. Dots mark sites of chemical synaptic output.

than b_4, the dendrites are thicker, and the dendritic arbor spreads more widely (extending beyond the series in both directions). The axon arbor is fairly flat and centred on the junction of strata 4 and 5. This arbor appears in tangential view to be markedly lobulated.

(*e*) *Synaptic patterns*

(i) *Outer plexiform layer*

We traced several b_1 and b_2 dendrites and one b_4 dendrite to their sites of contact with the cone pedicle. The b_1 dendrite always partially invaginated the pedicle and, forming its post-synaptic density, terminated well short of the synaptic ribbon (figure 10*a*). The b_2 dendrite fully invaginated the pedicle, forming its post-synaptic density immediately beneath the ribbon (figure 10*b*). This confirms Nelson & Kolb (1983) who termed these cells CB5 and CB6, respectively. The b_4 dendrite (figure 10*c*) fully invaginated the pedicle, forming its post-synaptic density just beneath the synaptic ribbon, like the b_2 dendrites.

We reconstructed (to the degree possible) the patterns of cone convergence onto all the bipolar cells in a retinal patch occupied by 35 cones. The next paper (Cohen & Sterling 1990*a*) presents the findings in detail, but we summarize here the points relevant to the issue of bipolar cell categories. The main sorting of cone bipolar cells according to patterns of cone input is

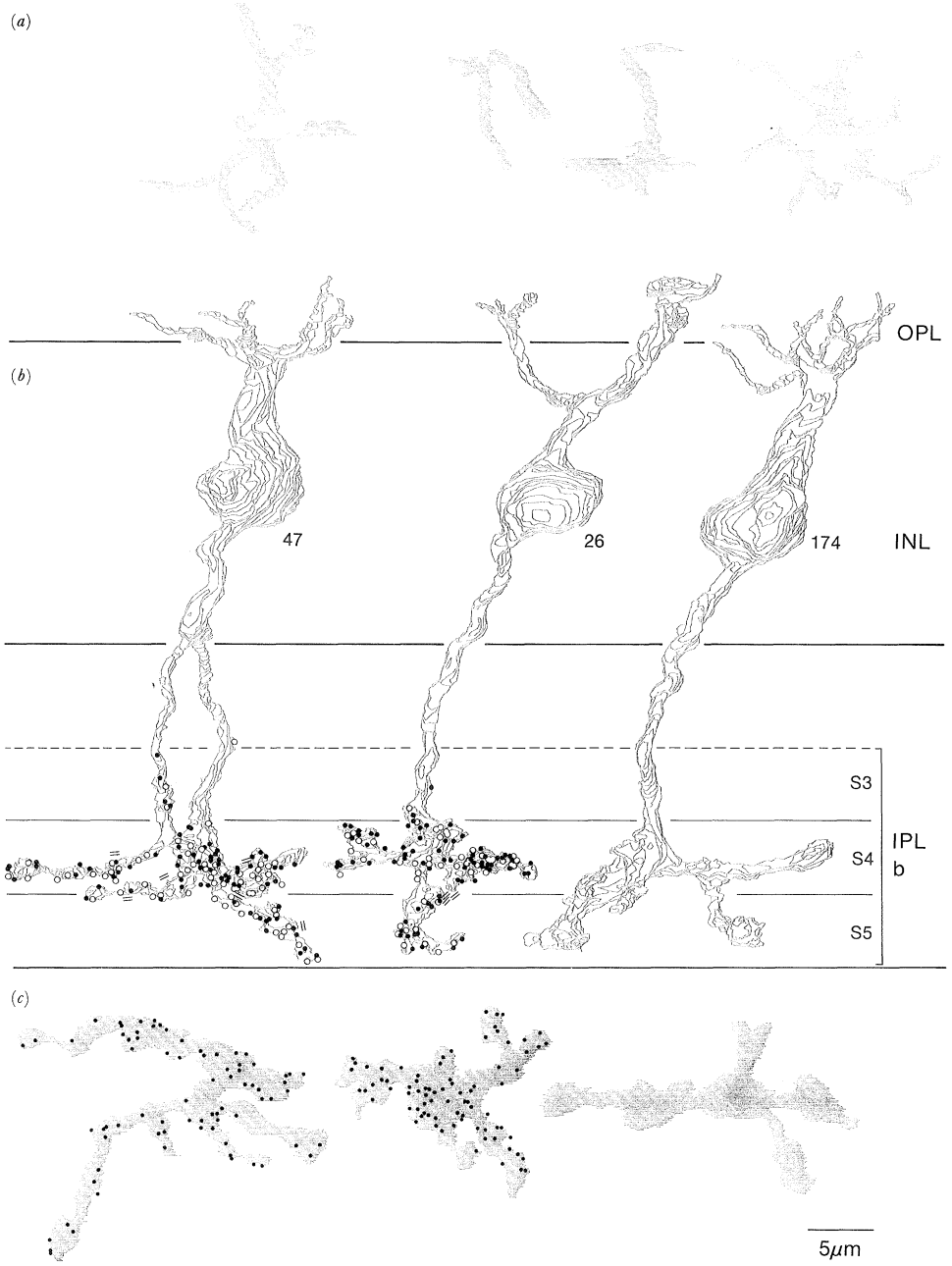

Figure 6. (*a*) Dendritic arbor of each cell in tangential view. (*b*) Reconstructions in vertical view of three b_2 bipolar neurons. (*c*) Axonal arbor of each cell in tangential view. Symbols as for figure 5.

into a wide-field cell that collect from no overlying cone pedicles (b_5) and narrow-field cells (b_1, b_2, b_4) that collect from all their overlying pedicles. Convergence onto the narrow-field cells varies from four to nine cones, and generally the broader b_2 and b_4 cells show greater convergence than the somewhat narrower b_1 cells. However, if one sorts the population of narrow-field cells according to differences in cone convergence, the categories created thereby would not correspond to those distinguished by morphology and soma position (figures 5–8).

Certain cells received 1–3 chemical synapses of the conventional kind, either on their dendrites or in one case on an axonal branch in the INL (figure 5). The presynaptic profiles were pale, and the synaptic junction was symmetrically dense. Most likely these contacts are from the interplexiform cell (Kolb & West 1977; Nakamura *et al.* 1980). Such contacts have been reported previously on the bipolars CBb_1 (McGuire *et al.* 1984; Sterling *et al.* 1988), and consistent with this we found them on b_1 bipolar cells (figure 5). A single pale contact was observed on a b_4 bipolar cell (no. 24 in figure 8).

(ii) *Inner plexiform layer*

We reconstructed for nine bipolar axons in sublamina *b* the full pattern of synaptic input and output. Ideally one would have wished to reconstruct the synaptic patterns for all of the bipolar cells in the patch, sort them on this basis, and see whether this sorting matches that based on morphology. Since this would have been unnecessarily slow, we reconstructed instead the synaptic patterns for two cells (where possible) of each category that had already been sorted

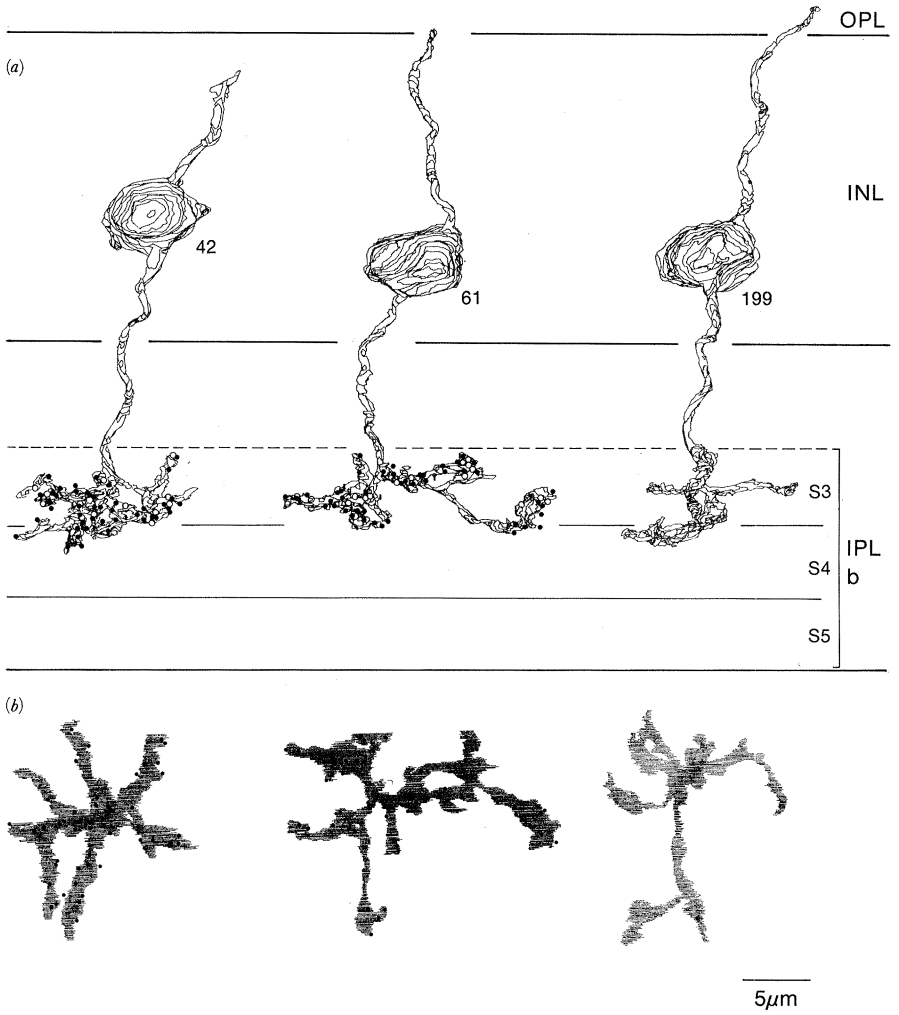

Figure 7. (*a*) Reconstructions in vertical view of three b_3 bipolar neurons. (*b*) Axonal arbor of each cell in tangential view. Symbols as for figure 5.

by morphology. The complete results are shown in tables 1–5; here we summarize the main points.

Inputs The number of amacrine synaptic contacts onto a bipolar axon varied between 15 and 75 (table 1). Cells in category b_3 differed from those in b_1, b_2, and b_4 in having markedly fewer amacrine contacts. We distinguished an amacrine contact as 'reciprocal' when it received a contact from the same bipolar axon (McGuire *et al.* 1984; Kolb 1979). The ratio non-reciprocal:reciprocal varied (0.75–2.00) from axon to axon for categories b_1–b_4, providing no means to distinguish between them. However, the ratio non-reciprocal:reciprocal for the b_5 axon was 24, and thus markedly different.

Outputs Each site of chemical synaptic output from a bipolar axon was marked on the pre-synaptic side by a 'ribbon' (Dowling & Boycott 1966; Kolb 1979; McGuire *et al.* 1984). The number of ribbons per axon varied by threefold between morphological categories (35–105). Cells within the same morphological category tended strongly to contain similar numbers of ribbons (table 2). Post-synaptic at each ribbon was a dyad, a pair of processes that could be either amacrine, or ganglion cell or both. The axons of categories b_1–b_3 divided their post-synaptic targets about equally between amacrine and ganglion cells; the b_5 axon preferred ganglion to amacrine cells (2:1), and b_4 axons preferred amacrines to ganglion cells (4:1) (table 2).

The post-synaptic ganglion cell profiles were further classified according to whether their cytoplasm was dark or pale. Previous work showed that usually dark profiles belong to β ganglion cells and pale profiles to α cells (McGuire *et al.* 1986). In the present material cone bipolar axons differed moderately in their relative contributions to dark and pale ganglion cell processes, but the variation was as great between axons of the same morphological category as between axons of different categories. The b_5 axon strongly preferred pale profiles to dark ones (8:1) (table 2), and it turned out, when these profiles were traced, that none belonged to α or β cells.

Each amacrine varicosity post-synaptic at a dyad was studied in successive sections to determine whether it was reciprocal, that is, feeding back to the bipolar axon, or non-reciprocal (McGuire *et al.* 1984; Freed *et al.* 1987). Here the variation within a morphological category was less than the variation between categories. The mean percentage of connections with reciprocal amacrine processes differed significantly between categories b_1, b_2, and b_3, and also between categories b_3 and b_4 (two-sample t test, $p < 0.05$). Thus sorting by

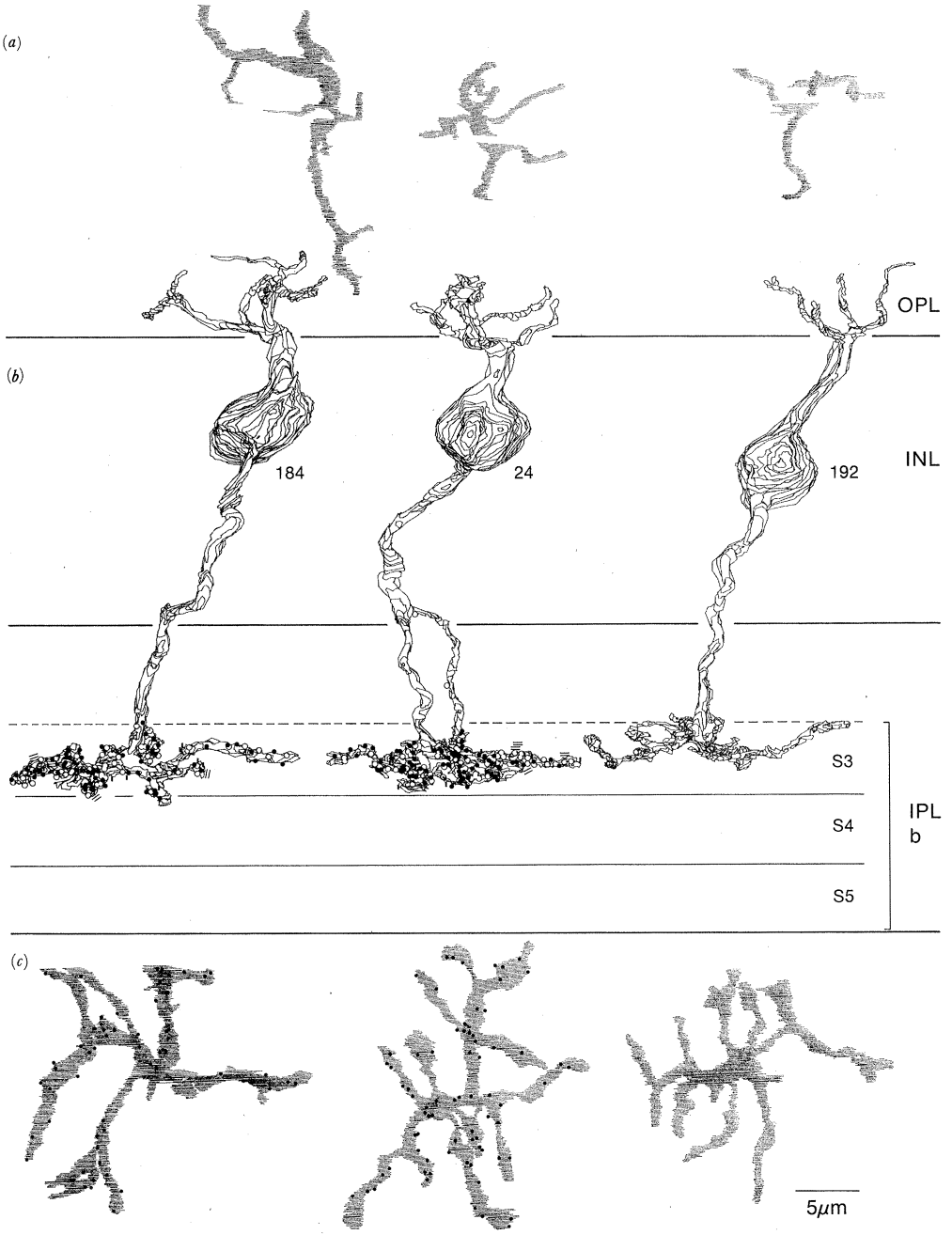

Figure 8. (*a*) Dendritic arbor of each cell in tangential view. (*b*) Reconstructions in vertical view of three b_4 bipolar neurons. (*c*) Axonal arbor of each cell in tangential view. Symbols as for figure 5.

this feature produces the same categories as sorting by the number of dyads and by morphology except that it does not separate categories b_1 and b_4. The b_2 axons contacted reciprocal and non-reciprocal amacrine processes about equally, while the b_1, b_3, and b_4 axons showed moderate preferences for non-reciprocal processes (non-reciprocal:reciprocal ratios between 5:1 and 2:1). The b_5 axon preferred non-reciprocal processes by a considerable margin (32:1).

One point that emerges from comparing tables 1 and 2 is that for each morphological category there seem to be fairly definite ratios of output sites to input sites. For categories b_1–b_4 these ratios are modest: 2.2, 1.3, 2.6, and 1.1. In contrast, the b_5 axon had a marked preponderance of output sites, the ratio being 17.5.

To summarize the several important respects in which the b_5 axon's synaptic organization differs from all the others: it has by far the fewest dyads and essentially no output to alpha or beta ganglion cells. It provides substantial output to amacrine cells, but receives very little input from them.

(iii) *Patterns of electrical synapse*

The cone bipolar axons commonly formed gap junctions (electrical synapses) with other processes. On the axons for which we studied the patterns of chemical synapses, we also studied the patterns of electrical synapses, measuring their areas and, where possible, identifying the processes to which the axons were coupled. The results are presented in table 3; here we summarize the main points.

Three out of the five categories of bipolar axon

PHILOSOPHICAL TRANSACTIONS OF THE ROYAL SOCIETY B BIOLOGICAL SCIENCES

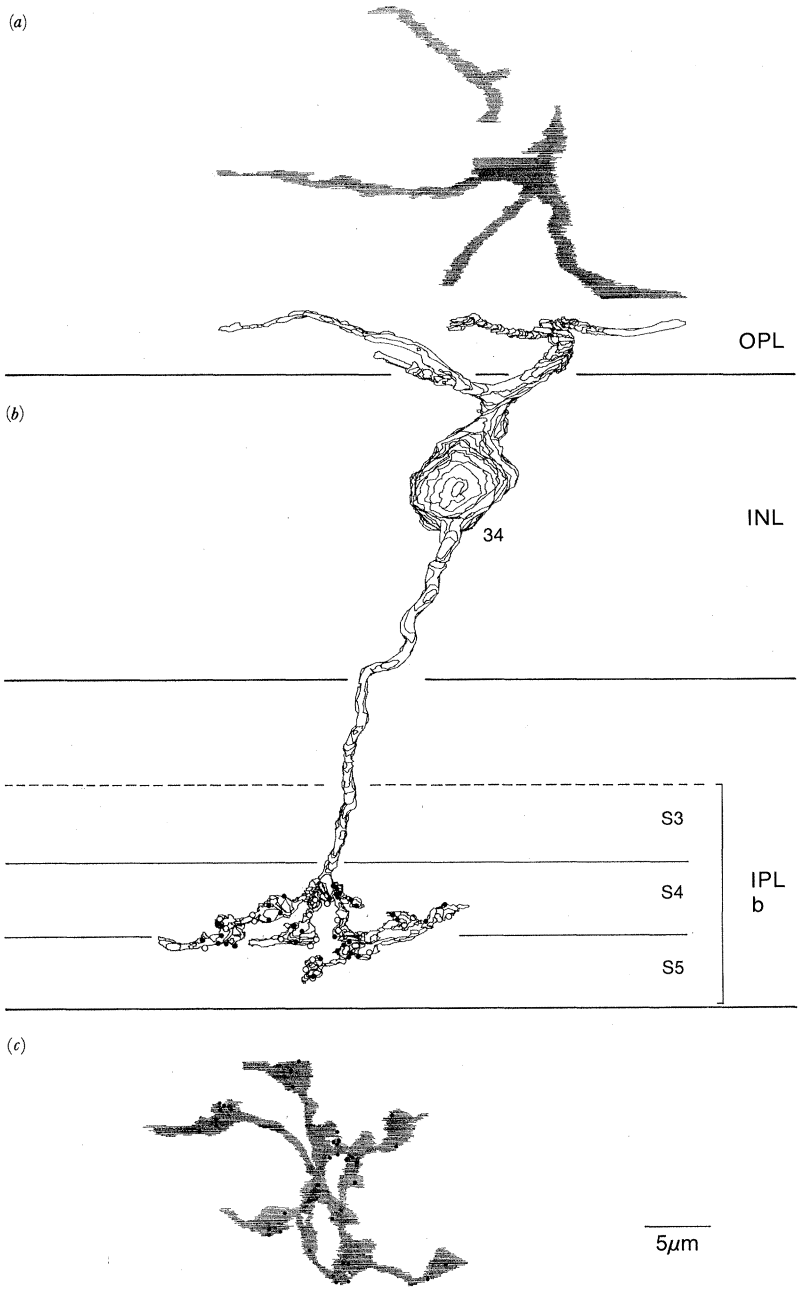

Figure 9. (*a*) Dendritic arbor in tangential view. (*b*) Reconstruction in vertical view of a b_5 bipolar neuron. (*c*) Axonal arbor in tangential view. Symbols as for figure 5.

formed gap junctions with branches of the AII amacrine cell. These were b_1 and b_2 (figures 11*a–c*), as already noted by McGuire *et al.* 1984, and b_4 (figure 11*d*). The b_1 junctions with the AII were numerous (about 10/b_1 axon) and large (mean = 0.44 μm^2). Most gap junctions on a given b_1 axon connected to a single AII cell, confirming previous observations (Sterling *et al.* 1988). The b_2 and b_4 gap junctions with the AII cell were fewer (about 4–5 per axon) and smaller (mean = 0.14 μm^2).

Two out of the five categories of bipolar axon formed gap junctions with branches of other bipolar axons. The b_4 axons were coupled to each other (figures 12*b*, *c*) through small junctions (mean = 0.05 μm^2), and the b_3 axons were coupled in this way to b_4 axons (figure 12*a*) through small junctions (mean = 0.03 μm^2). Thus although the b_3 is not directly coupled to the AII cell, it seems to be coupled indirectly to the AII by way of the b_4 axon. The b_5 axon was the only one that was not found to be coupled to the AII cell.

(iv) *Sorting by synaptic pattern*

When patterns of chemical and electrical connections were considered together, there was enough information to sort the nine bipolar cells into the same five categories as determined by morphology: b_1 cells had more ribbons (dyads) and larger AII gap junctions than b_2 cells; b_2 cells lacked gap junctions with other bipolar axons that were formed by b_3 and b_4 cells; b_3

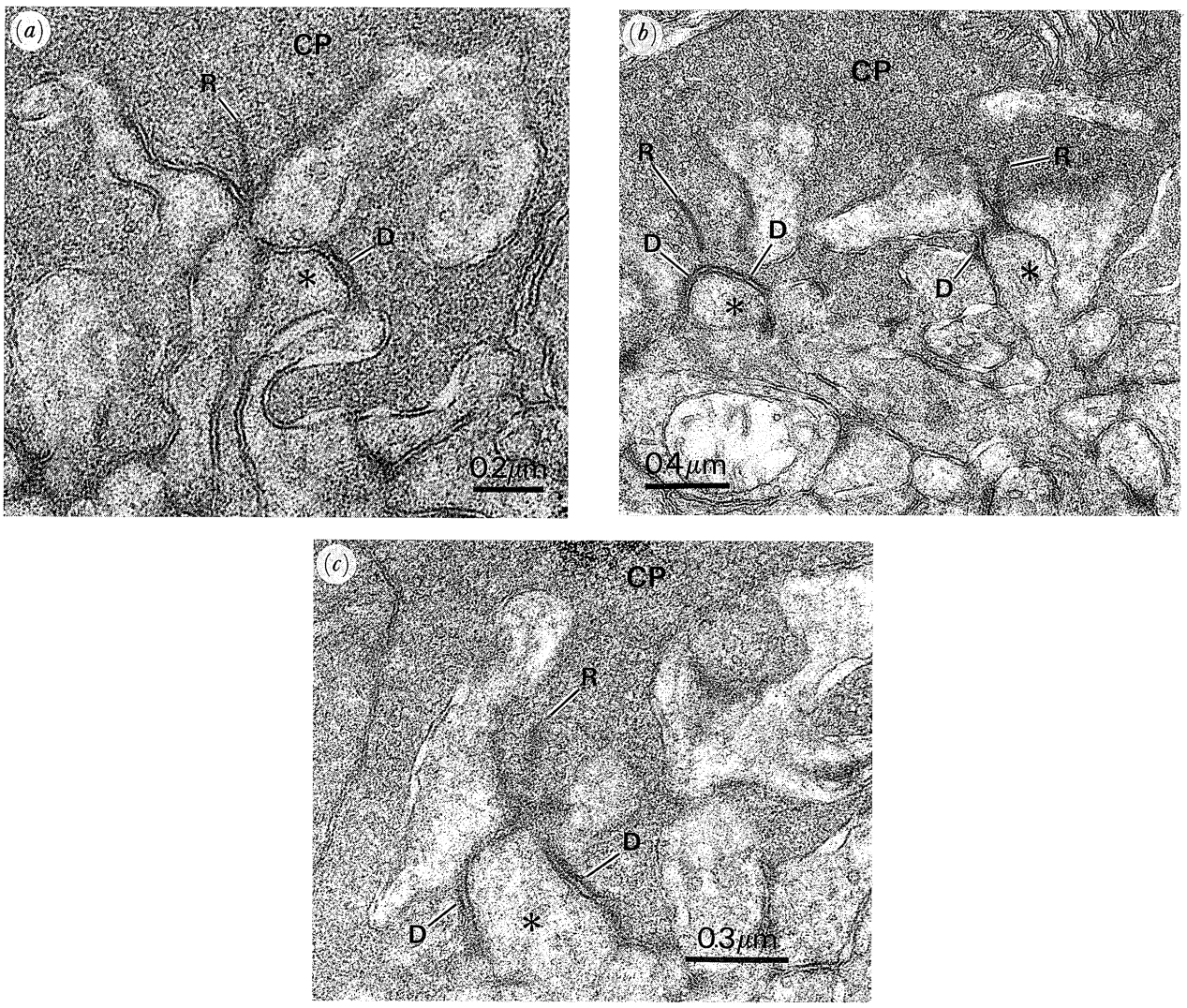

Figure 10. Electron micrographs of synaptic contacts between cone pedicle and bipolar dendrites. (*a*) b_1 dendrite (*) pushes part way into the pedicle ('semi-invaginating') and is post-synaptic to cone at site (D) some distance from the ribbon. Another dendrite, unidentified as to type, terminates just beneath the ribbon ('fully invaginating'). R, ribbon; CP, cone pedicle. (*b*) Two thorns (*) from a single b_2 dendrite invaginate a cone pedicle fully and form post-synaptic density just beneath the synaptic ribbon. (*c*) b_4 dendrite fully invaginates the cone pedicle to form post-synaptic density just beneath the ribbon and also a density (D) at some distance from the ribbon.

Table 1. *Inputs (chemical synapses) to cone bipolar axons from amacrine cells*

	b_1		b_2		b_3		b_4		b_5
cell number	182	38	47	26	42	61	184	24	34
number of contacts	47	49	75	51	15	22	54	63	25
reciprocal	40%	33%	48%	57%	40%	55%	41%	46%	4%
non-reciprocal	60%	67%	52%	43%	60%	45%	59%	54%	96%

Table 2. *Outputs (chemical synapses) from cone bipolar axons to amacrine and ganglion cells*

	b_1		b_2		b_3		b_4		b_5
cell number	182	38	47	26	42	61	184	24	34
number of dyads	105	105	78	82	47	48	60	73	35
amacrine cells	42%	46%	44%	51%	38%	55%	72%	71%	30%
ganglion cells	48%	46%	49%	41%	50%	38%	20%	16%	60%
unidentified	10%	8%	7%	8%	12%	7%	8%	13%	10%
ganglion cells:									
dark	73%	54%	82%	63%	56%	55%	35%	50%	7%
pale	27%	46%	18%	37%	44%	45%	65%	50%	93%
amacrine cells:									
reciprocal	24%	23%	55%	43%	16%	22%	29%	31%	3%
non-reciprocal	76%	77%	45%	57%	84%	78%	71%	69%	97%

PHILOSOPHICAL TRANSACTIONS OF THE ROYAL SOCIETY B BIOLOGICAL SCIENCES

Table 3. *Gap junctions (GJs) formed by cone bipolar synapsis*

	b_1			b_2			b_3		b_4	
cell number with AII:	182	38	213	47	26	174	42	61	184	24
no. GJs	11	10	8	6	3	6	0	0	4	4
total area (μm^2)	4.5	5.1	3.3	0.5	0.5	1.0			0.76	0.33
with b_3:										
no GJs	0	0	0	0	0	0	0	0	6	4
total area (μm^2)									0.21	0.12
with b_4:										
no. GJs	0	0	0	0	0	0	4	5	6	5
total area (μm^2)							0.11	0.19	0.32	0.23
unidentified:										
no. GJs	0	0	0	0	0	0	3	1	4	3
total area (μm^2)							0.09	0.03	0.22	0.17

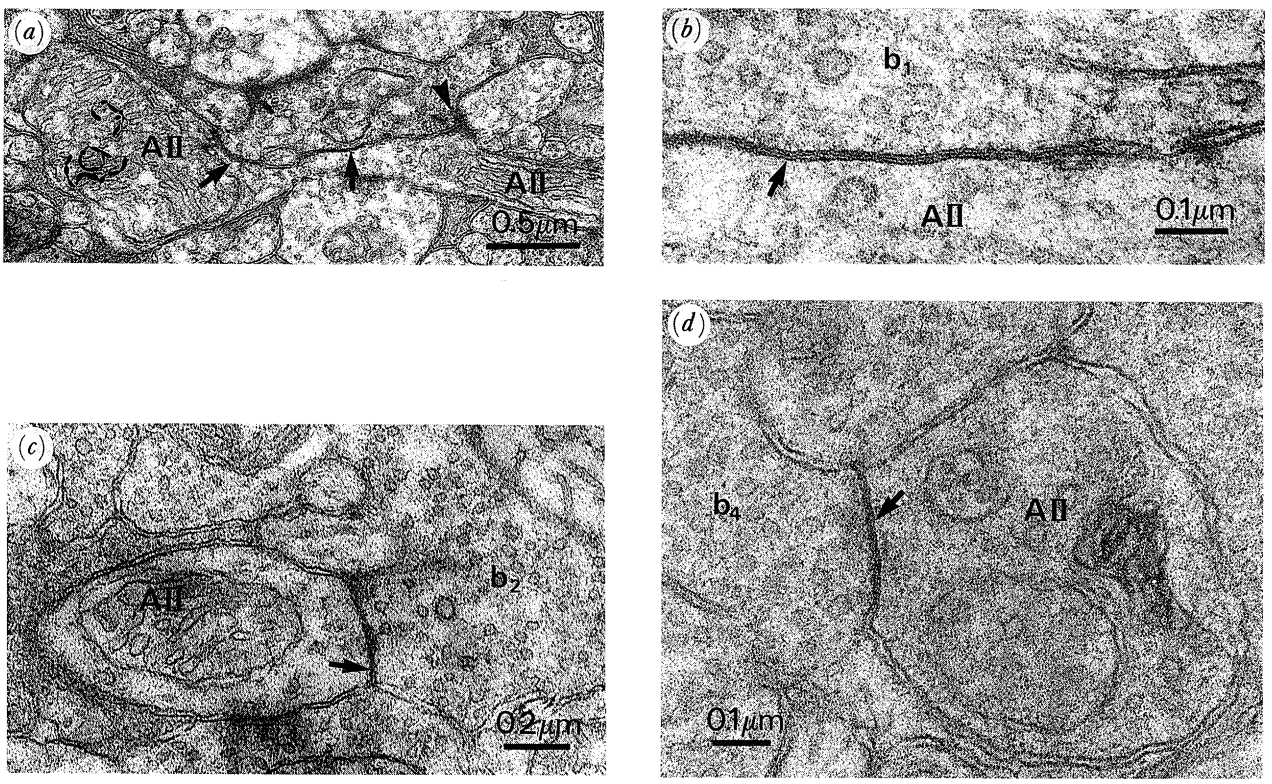

Figure 11. Gap junctions between cone bipolar axons and AII amacrine processes. (*a*) b_1 axon (note ribbon) forms two gap junctions (arrows) with AII. b_1 axon also provides a chemical synapse (arrowhead) to the AII cell. This connection was exceptional (because most bipolar chemical synapses to the AII derived from the rod bipolar) and only two other examples of b_1–AII chemical synapse were observed. (*b*) b_1–AII gap junctions at higher magnification. (*c*) b_2–AII gap junction. (*d*) b_4–AII gap junction.

cells lacked gap junctions with AII cells and with other members of its own category, both of which were formed by b_4 cells; the b_5 was distinguished by its total lack of gap junctions as well as by multiple, unique patterns of chemical synapse mentioned above.

Stratification of chemical synaptic connections The sites of chemical synaptic input and output on each axon were mainly restricted to the strata of their arborization (figures 5–9). We determined for each axon the percentage of its input and output in each stratum (table 4). This was both fairly constant and somewhat distinctive for each morphological category. Thus sorting the cells by the stratification of their inputs and outputs is consistent with the categories derived from morphology and synaptic pattern.

Sorting the rest of the cells The issue then arose: given that 13 cells had been sorted by morphology into five categories (figures 5–9) and that nine of these had been sorted by synaptic pattern into the same five categories (tables 1–4), would the remaining 29 bipolar neurons in the population also distribute neatly in the same way? Just as plausibly, the 29 cells might create additional categories, or they might, by filling in the gaps in parametric space, obliterate the categories developed from the samples.

As anticipated from the 13 cells reconstructed in detail, no single parameter would sort the cells. Indeed, the two parameters most easily measured, axon diameter (see figure 13) and soma depth, when plotted separately (figure 14, see tick marks) showed no

PHILOSOPHICAL TRANSACTIONS OF THE ROYAL SOCIETY B BIOLOGICAL SCIENCES

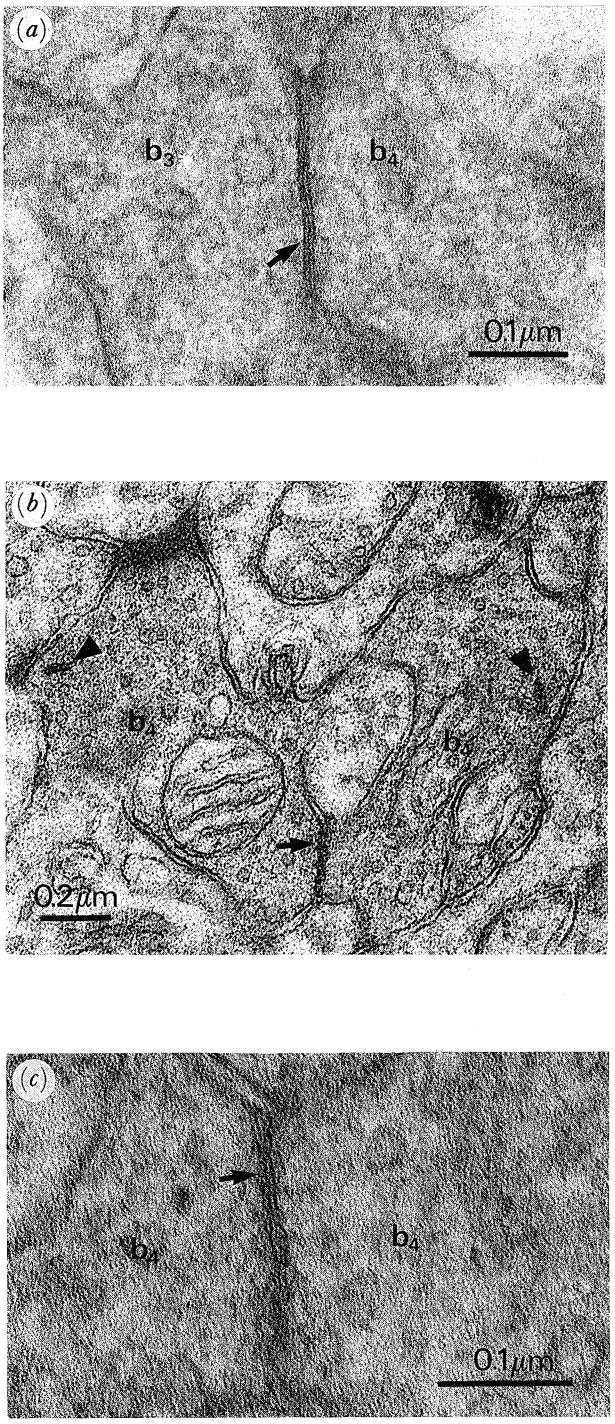

Figure 12. Gap junctions between bipolar axons. (*a*) Gap junction between b_3 and b_4 processes. (*b*) Two b_4 processes (arrowheads mark synaptic ribbons) form gap junction (arrow). (*c*) Higher magnification of same junction in the adjacent section.

obvious clusters. Even when the two parameters were plotted jointly, (figure 14, scatter plot), no definite clusters appeared. Adding a third parameter, 'total area of gap junctions with AII amacrine cells' (figure 15), revealed several distinct clusters: six cells with extensive AII gap junctions were labelled by *1s* in the plot because their cluster included the reconstructed neurons termed b_1 (figure 5); nine cells lacking any AII gap junctions were labelled *3s* in the plot because their cluster included the reconstructed neurons termed b_3 (figure 7). A group of 10 cells remained (*2s*, *4s* in figure 15) that were separated from *1s* and *3s* by these three parameters but not from each other. However, adding a fourth parameter, 'gap junctions with other bipolar cells' (circled cells in figure 15) produced two new clusters. Cells in these clusters were labelled, respectively, b_4 and b_2 because they included the cells so classified by detailed reconstruction (figures 6 and 8).

Another parameter, 'stratification index', separated the cells into two major groups (figure 16) but by itself did not define any smaller clusters. However, with additional information as to which cells make gap junctions with the AII amacrine cell and whether these junctions are large or small, the familiar set of clusters emerged once more (figure 16).

The multiparametric plots of figures 15 and 16 include, respectively, 25 cells and 23 cells, almost double the number reconstructed in detail. Thus, to our original questions, 'would enlarging the sample size create additional categories or obliterate existing ones?', the answers are clearly, 'no'. The categories b_1–b_5, defined first by detailed reconstruction of a few cells, also emerge naturally among a larger number of cells when they are viewed in multiparametric space. Further, the same categories emerge even when the parameter spaces are somewhat different (figures 15 and 16). The only criterion for selecting the additional cells was that they lie near the middle of the series. This insured that the cells would be complete, so that their comparison to the reconstructed cells would be valid.

We wished to classify the remaining 17 cells, mainly to study the mosaic distribution of each morphological category. However, the data that could be gathered for these cells tended to be fragmentary: eight cells had their axons within the series, but their somas and dendritic arborizations had been cut away; 10 cells had axons so near the edge of the series that observations were incomplete (figure 2). Where, for example, only half the axon arbor was present, it was impossible to determine reliably its stratification index or its total area of gap junctions with the AII amacrine.

Table 4. *Stratification of chemical synaptic connections in sublamina b*

		b_1		b_2		b_3		b_4		b_5
cell number		182	38	47	26	42	61	184	24	34
% input to:	S3	6	7	4	4	80	95	96	100	0
	S4	26	52	77	77	20	5	4	0	56
	S5	64	41	19	19	0	0	0	0	44
% output to:	S3	15	22	5	10	72	79	93	99	0
	S4	36	50	78	73	28	21	7	1	62
	S5	49	28	17	17	0	0	0	0	38

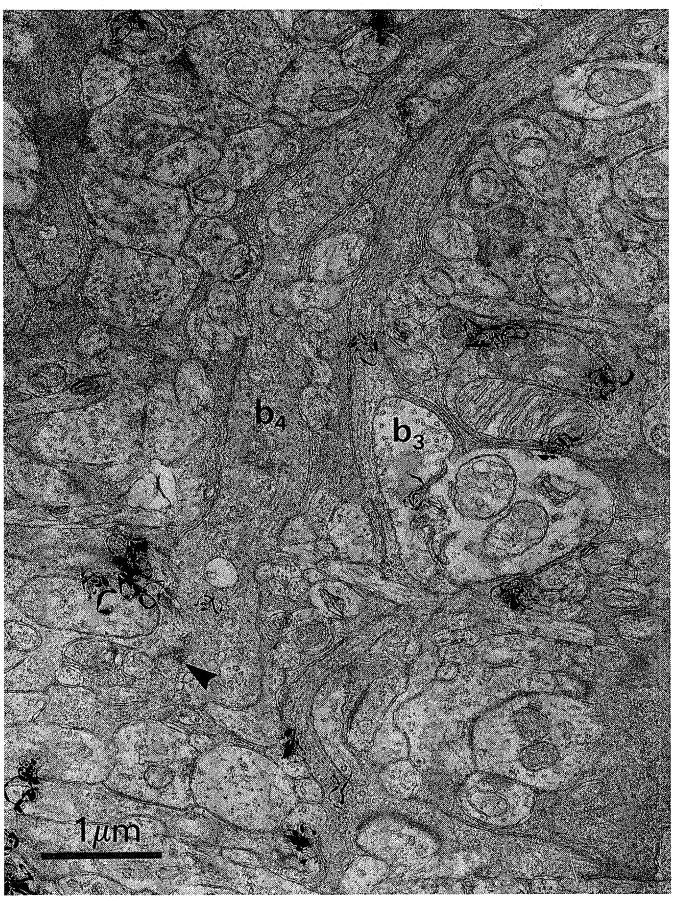

Figure 13. Electron micrograph of adjacent cone bipolar axons. The b_3 axon (cell 199; see figure 7) is thin; the b_4 axon (cell 192; see figure 8) is thicker. Arrowhead points to synaptic ribbon in b_4 axon.

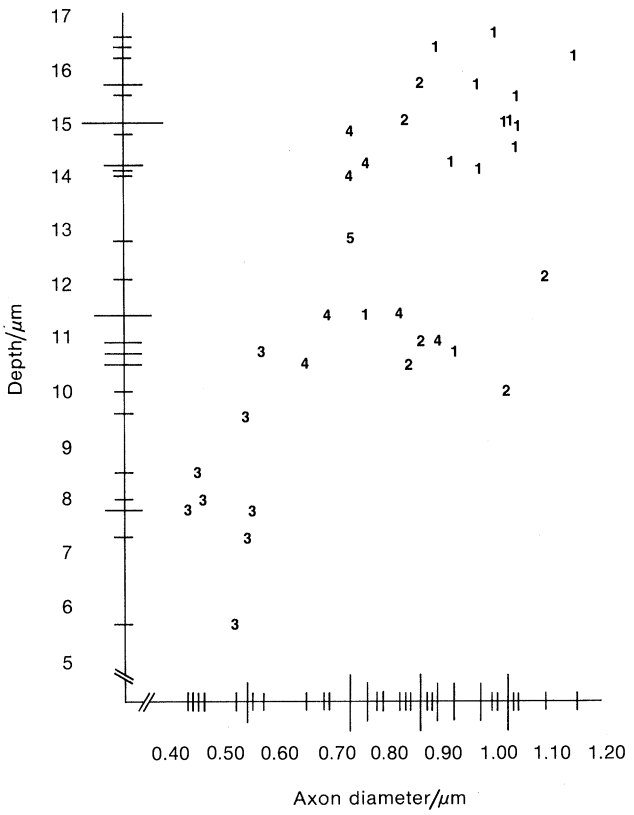

Figure 14. Tick marks along either axis represent distribution of diameter (42 axons) and depth (34 somas). Scatterplot represents joint distribution of these two parameters. No cluster emerges distinctly.

Thus the remaining 17 cells could only be classified according to progressively more limited sets of criteria, and these are shown in table 5.

To place three incomplete cells into the group that included b_3 and b_4 was straightforward: if a cell formed even one gap junction with another bipolar axon, it could belong only to this broad group. Then, if a cell in this group showed even a single AII gap junction, it could only be a b_4. Furthermore, b_3*s* and b_4*s* could also be separated by axon diameter which was measured for every cell in the population.

This left seven incomplete cells in the group that included b_1*s* and b_2*s*. To assign an incomplete cell to one of these categories was harder because the cells overlapped in axon diameter, stratification index, and presence of gap junctions with AII amacrines. Where an axon was incomplete, its total gap junction area with AIIs could not be assessed. Then the only remaining criterion was whether the observed gap junctions were large (b_1) or small (b_2). Consequently, the last few positive identifications (table 5) became shakier. Still, no evidence of additional categories appeared.

Mosaic features Satisfied that each category (b_1–b_5) represents a natural cluster, rather than an arbitrary one such as might be produced by a 'splitter', we considered how each category was distributed in the retinal mosaic. These distributions (figure 17) were fairly even. They were also fairly dense with b_1's distribution being slightly denser than the others. The

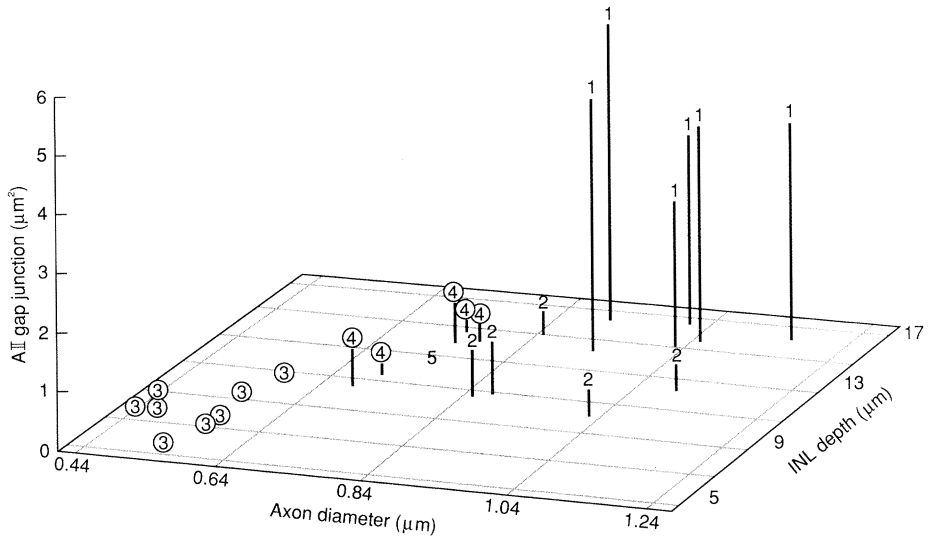

Figure 15. Distribution of 25 cone bipolar cells in a four-dimensional parametric space. Circles show gap junctions with other bipolar cells. As shown in figure 14, the distribution of cells according to axon diameter (x-axis) is continuous, as is the distribution according to depth in the INL (z-axis). The distribution of cells according to the size of their gap junctions with AII amacrine processes (y-axis) is essentially bimodal, as is the distribution according to the presence of gap junctions with other bipolar cells (circled cells). We number the clusters that emerge naturally in this 4-D space b_1–b_5 because they correspond to the clusters that emerge from comparing their morphologies (figures 5–9) and synaptic patterns (tables 1–5).

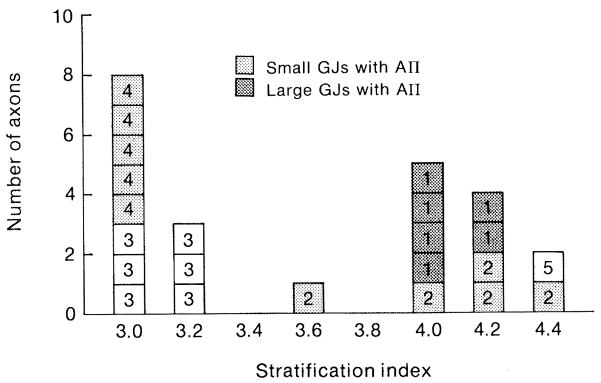

Figure 16. Histogram: distribution of 23 cone bipolar neurons in three-parameter space. Stratification index sorts population into two broad groups. AII gap junctions (two sizes) sorts each group into smaller clusters corresponding to those identified in figure 15. To compute a cell's 'stratification index', the fraction of its axon arbor distributed to each stratum was estimated to the nearest one fifth. The estimate was multiplied by the stratum number (3, 4 or 5) and the result summed for all three strata.

mean distance to a nearest neighbour for each category ranged from 10.3 ± 2.5 μm to 13.8 ± 3.5 μm (figure 17) and every cell was closer to members of other categories than to members of its own category. This was not a criterion for classification, but it should certainly be true if the classifications were all correct. The 'coverage factor' for each category (distribution density X area of axonal field; Wässle *et al.* 1978) was in each case close to one.

DISCUSSION

(*a*) *Types*

The 42 bipolar neurons studied here comprise all the cone bipolar neurons in this patch of retina that innervate sublamina *b*. When large subsets of this population are plotted in multiparametric space (figures 15 and 16), the cells sort cleanly into five definite clusters with no evidence of intermediate forms. Furthermore, when the cells are sorted by different sets of features, such as morphology (figures 5–9) and synaptic pattern (tables 1–5), the same clusters emerge. Although morphology and synaptic pattern could not be fully reconstructed for every cell, the selected features that were studied for the complete population provided no hint of intermediate forms. Thus the categories b_1–b_5 emerge naturally, rather than from arbitrary 'splitting' or 'lumping'. In all of these respects they satisfy the criteria for natural cell 'types' (Rodieck & Brening 1983; Sterling 1983), and henceforth we shall so refer to them.

(*b*) *Other studies*

The cell types shown here agree to a certain extent with those proposed by others. Thus our types b_1 and b_2 correspond in all respects to those called CBb_1 and CBb_2 by McGuire *et al.* (1984) in their study that used the same method at the same eccentricity. The cells we call b_3 do *not* resemble the one that McGuire *et al.* (1984) called CBb_3. We believe that the latter cell was actually a b_1 cell incompletely reconstructed because of the limited length of that series. Consistent with this is the cell's arborization in strata 3–5, its large gap junctions with AII processes, and its interplexiform contacts. McGuire *et al.* (1984) did not find the types we call b_3 and b_4, probably because their study included too few cells in sublamina *b*. We have since returned to the series prepared for that study and confirmed the presence of these two types. There was

Table 5. *Cone bipolar features for multiparametric classification*

I.D. number	depth INL (μm)	Axon diam (μm)	Strat. index	GJs with CBs	no. GJs with AII	total area (μm²) AII GJs	AII GJ (μm²) ($\bar{x}\pm$s.d.)	cell type
38	16.4	0.90	4	N	10	5.07	0.51±0.37	b_1
182	16.2	1.16	4.2	N	11	3.65	0.41±0.26	b_1
213	16.6	1.01	4	N	8	3.30	0.41±0.28	b_1
5	15.0	1.03	4	N	9	2.45	0.27±0.14	b_1
49	14.2	0.93	—	N	9	4.31	0.48±0.24	b_1
48	15.5	1.05	—	N	13	3.81	0.29±0.16	b_1
230	—	0.80	4.2	N	5	—	—	b_1
27	15.0	1.04	4	N	8	—	—	b_1
141	15.0	1.03	—	N	10	—	—	b_1
168	11.4	0.77	—	N	5	—	—	b_1
164	14.1	0.98	—	N	6	—	—	b_1
60	10.7	0.93	—	N	1	—	—	b_1
147	15.7	0.98	—	N	3	—	—	b_1
231	—	0.89	—	N	6	—	—	b_1
174	10.9	0.87	4.4	N	6	0.94	0.16±0.09	b_2
26	10.0	1.03	4.2	N	3	0.52	0.17±0.03	b_2
47	12.1	1.10	4.2	N	6	0.49	0.08±0.04	b_2
143	15.0	0.84	—	N	3	0.47	0.09±0.03	b_2
81	10.5	0.85	—	N	4	0.85	0.21±0.19	b_2
158	15.7	0.87	—	N	1	—	—	b_2
232	—	0.79	4	N	3	—	—	b_2
234	—	1.00	3.6	N	6	—	—	b_2
233	—	0.87	—	N	2	—	—	b_2
42	8.5	0.46	3.2	7	0	0	—	b_3
61	5.7	0.53	3	6	0	0	—	b_3
3	8.0	0.47	3.2	Y	0	0	—	b_3
199	7.8	0.44	3.2	Y	0	0	—	b_3
88	9.6	0.55	3	Y	0	0	—	b_3
142	10.7	0.58	3	Y	0		—	b_3
35	7.8	0.56	—	Y	0	0	—	b_3
156	7.3	0.55	—	Y	0	0	—	b_3
235	—	0.45	—	Y	0	0	—	b_3
24	14.2	0.77	3	12	4	0.33	0.08±0.04	b_4
184	14.0	0.74	3	16	4	0.76	0.19±0.07	b_4
104	10.5	0.68	3	Y	4	0.68	0.14±0.12	b_4
192	11.4	0.70	3	Y	3	0.26	0.09±0.02	b_4
194	14.8	0.74	—	Y	2	0.21	0.10±0.05	b_4
162	10.9	0.90	—	Y	1	—	—	b_4
212	11.4	0.83	—	Y	1	—	—	b_4
236	—	0.69	3	Y	1	—	—	b_4
237	—	0.88	—	Y	2	—	—	b_4
34	12.8	0.74	4.4	N	0	0	—	b_5

no example of type b_5, probably because its distribution is sparse, and the series was relatively short.

The correspondence to typologies based on Golgi impregnation are less certain because comparison at the same eccentricity and in the same plane of view are unavailable. Thus while the cells we call b_1 and b_2 may correspond to those called CBb1 and CBb2 by Pourcho & Goebel (1987), certain details do not entirely match. For example, the axons of our b_1 and b_2 cells arborize substantially in all strata of sublamina *b* whereas the possibly corresponding cells shown by Pourcho & Goebel (1987) in their figure 4 have rather flat arborizations virtually restricted to stratum 4. Further evidence of such flat arbors is also given in their table 2. Where synaptic pattern as well as morphology can be compared, one can be more confident of the correspondences. Thus our b_1 and b_2 cells certainly correspond to those called cb5 and cb6 by Kolb *et al.* (1981) and Nelson & Kolb (1983). Our type b_5, as the only wide-field cell, most likely corresponds to the wide-field cell called CBb5 by Pourcho & Goebel (1987), cb8 by Kolb *et al.* (1981), and wb by Famiglietti (1981).

A probable true difference from previous reports is that whereas Golgi studies (Kolb *et al.* 1981; Pourcho & Goebel 1987) describe only one category of cell with axon arborization restricted to stratum 3, we present evidence for two types, b_3 and b_4. We believe that in this case, the Golgi method either failed to impregnate one of the types or that the morphological differences between the types (compare our figures 7 and 8) are so subtle as to be lost in the 'noise' of variation between retinas and between different loci in the same retina. Finally, a bipolar cell with a bistratified axon has been

PHILOSOPHICAL TRANSACTIONS OF THE ROYAL SOCIETY B BIOLOGICAL SCIENCES

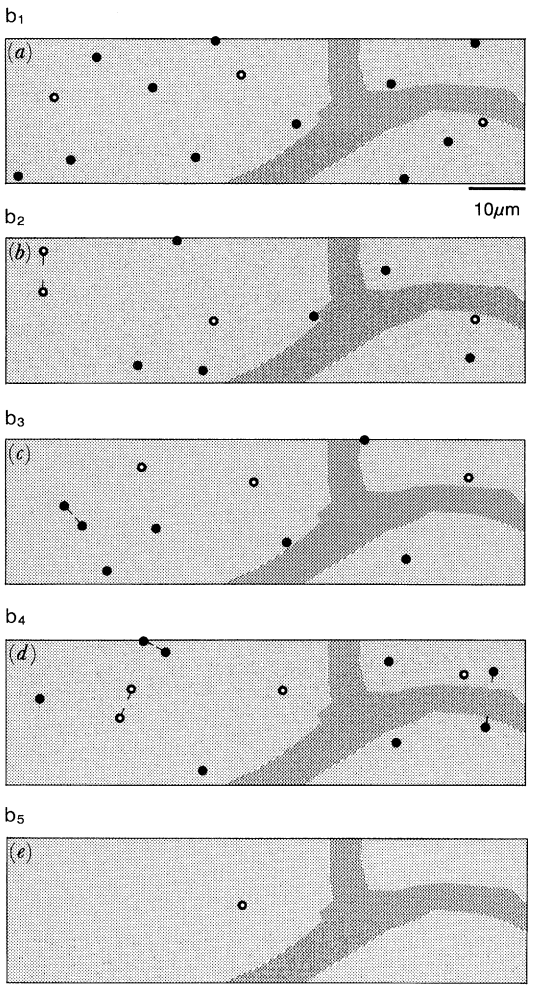

Figure 17. Location in tangential plane, according to cell type of all 42 cone bipolar axons that arborize in sublamina *b*. Open circles show cells that were reconstructed. Paired circles with tick marks show bifurcation from the parent axon (see, for example cell 47, figure 6; cell 24, figure 8). Shaded area shows blood vessel at junction of sublamina *a* and *b*. (*a*) Cell density = 6100 mm^{-2}; nearest neighbour distance = 10.3 ± 2.5 μm. (*b*) Cell density = 4000 mm^{-2}; nearest neighbour distance = 12.1 ± 5.2 μm. (*c*) Cell density = 4400 mm^{-2}; nearest neighbour distance = 13.8 ± 3.5 μm. (*d*) Cell density = 4300 mm^{-2}; nearest neighbour distance = 13.1 ± 3.7 μm. (*e*) Cell density = *ca.* 450 mm^{-2}.

identified by Golgi impregnation (called CBb3 by Pourcho and Goebel (1987) and cb4 by Kolb *et al.* (1981)). No cell with this morphology was present in the patch of retina studied here; perhaps, as suggested by these authors, it is restricted to more peripheral retina.

(*c*) *Significance*

Given the basically good agreement with the Golgi work, it is fair to ask, what of significance has been added by the considerable effort of our study? What the Golgi method contributes are hypotheses: broadly, that retinal neurons belong to discrete categories, and narrowly, that particular examples deserve to have categories organized around them. To prove these hypotheses requires morphological evaluation of the whole population in a specific area, so as to test whether the differences between the impregnated (or injected) examples truly represent discrete differences between subpopulations. For example, the ganglion cell categories, 'alpha' and 'beta', were hypothesized from Golgi impregnations (Boycott & Wässle 1974) and later proved rigorously to represent true 'types' in a series of studies that included the whole population (Wässle *et al.* 1975; Wässle *et al.* 1981*a*, *b*). The corresponding proof for the cone bipolar types that innervate sublamina *b* is one contribution of the present study.

Another contribution is the mapping of natural types onto the whole population of bipolar cells. Thus we now know for sublamina *b* just how many of the 19000 cone bipolar axons per square millimetre belong to each type; furthermore we know for each type the spacing (figure 17) and the axonal coverage factor. Finally, by identifying in this material every sublamina *b* bipolar cell by type, we set the stage for subsequent tracing of their circuitry in the outer and inner plexiform layers. Such studies, described in the companion paper (Cohen & Sterling 1990*a*) and elsewhere (Cohen & Sterling 1990*b*, *c*), lead to the surprising conclusion that each cone is the source of about 10 qualitatively distinct parallel pathways to the inner plexiform layer, three of which converge upon the *on*-beta ganglion cell.

We thank Dave Carter, Sam Hong, and Ellen Magyarits for technical assistance, Suzanne Leahy for artwork, and especially Maria Koebert for extensive contributions to preparing the manuscript. We are grateful to Professors Ed Pugh, R. W. Rodieck, and B. Boycott for many suggestions. Supported by NIH grants EY00828 and EY07035.

REFERENCES

Boycott, B. B., Peichl, L. & Wässle, H. 1978 Morphological types of horizontal cell in the retina of the domestic cat. *Proc. R. Soc. Lond.* B **203**, 229–245.

Boycott, B. B. & Kolb, H. 1973 The connections between the bipolar cells and photoreceptors in the retina of the domestic cat. *J. Comp. Neurol.* **148**, 91–114.

Boycott, B. B. & Wässle, H. 1974 The morphological types of ganglion cells of the domestic cat's retina. *J. Physiol. Lond.* **240**, 397–419.

Cohen, E. & Sterling, P. 1986 Accumulation of (3H) glycine by cone bipolar neurons in the cat retina. *J. Comp. Neurol.* **250**, 1–7.

Cohen, E. & Sterling, P. 1990*a* Convergence and divergence of cones onto bipolar cells in the central area of cat retina. *Phil. Trans. R. Soc. Lond.* B **330**, 323–328.

Cohen, E. & Sterling, P. 1990*b* Microcircuitry for the receptive field center of the on-beta ganglion cell. *J. Neurophysiol.* (In the press.)

Cohen, E. & Sterling, P. 1990*c* Parallel pathways from cones to the on-beta ganglion cell. (Submitted.)

Dowling, J. E. & Boycott, B. B. 1966 Organization of the primate retina: electron microscopy. *Proc. R. Soc. Lond.* B **166**, 80–111.

Famiglietti, E. V. Jr. 1981 Functional architecture of cone bipolar cells in mammalian retina. *Vision Res.* **21**, 1559–1563.

Famiglietti, E. V. Jr. & Kolb, H. 1976 Structural basis for on- and off-center responses in retinal ganglion cells. *Science, Wash.* **194**, 193–195.

PHILOSOPHICAL TRANSACTIONS OF THE ROYAL SOCIETY B BIOLOGICAL SCIENCES

Fisher, S. & Boycott, B. 1974 Synaptic connexions made by horizontal cells within the outer plexiform layer of the retina of the cat and the rabbit. *Proc. R. Soc. Lond.* B **186**, 317–331.

Freed, M. A., Smith, R. & Sterling, P. 1987 Rod bipolar array in the cat retina: Pattern of input from rods and GABA-accumulating amacrine cells. *J. Comp. Neurol.* **266**, 445–455.

Freed, M. A. & Sterling, P. 1988 The On-alpha ganglion cell of the cat retina and its presynaptic cell types. *J. Neurosci.* **8**, 2303–2320.

Kolb, H. 1974 The connections between horizontal cells and photoreceptors in the retina of the cat: electron microscopy of Golgi preparations. *J. Comp. Neurol.* **155**, 1–14.

Kolb, H. 1979 The inner plexiform layer in the retina of the cat: Electron microscopic observations. *J. Neurocytol.* **8**, 295–329.

Kolb, H., Nelson, R. & Mariani, A. 1981 Amacrine cells, bipolar cells, and ganglion cells of the cat retina: a Golgi study. *Vision Res.* **21**, 1081–1114.

Kolb, H. & West, R. W. 1977 Synaptic connections of the interplexiform cell in the retina of cat. *J. Neurocytol.* **6**, 155–170.

McGuire, B. A., Stevens, J. K. & Sterling, P. 1984 Microcircuitry of bipolar cells in cat retina. *J. Neurosci.* **4**, 2920–2938.

McGuire, B. A., Stevens, J. K. & Sterling, P. 1986 Microcircuitry of beta ganglion cells in cat retina. *J. Neurosci.* **6**, 907–918.

Nakamura, Y., McGuire, B. A. & Sterling, P. 1980 Interplexiform cell in cat retina: identification by selective uptake of (3H)-GABA. *Proc. natn Acad. Sci. U.S.A.* **77**, 658–661.

Nelson, R. & Kolb, H. 1983 Synaptic patterns and response properties of bipolar and ganglion cells in the cat retina. *Vision Res.* **23**, 1183–1195.

Pourcho, R. G. & Goebel, D. J. 1987 A combined Golgi and autoradiographic study of 3H-glycine-accumulating cone bipolar cells in cat retina. *J. Neurosci.* **7**, 1178–1188.

Rodieck, R. W. & Brening, R. K. 1983 Retinal ganglion cells: Properties, types, genera, pathways and trans-species comparisons. *Brain Behav. Evol.* **23**, 121–164.

Rodieck, R. W. 1989 Starburst amacrine cells of the primate retina. *J. Comp. Neurol.* **285**, 18–37.

Smith, R. G. 1987 Montage: A system for three-dimensional reconstruction by personal computer. *J. Neurosci. Meth.* **21**, 55–69.

Steinberg, R. H., Reid, M. & Lacy, P. L. 1973 The distribution of rods and cones in the retina of the cat (*Felis domesticus*). *J. Comp. Neurol.* **148**, 229–248.

Sterling, P. 1982 Identified neurons in the cat retina. In *Changing concepts of the nervous system* (ed. A. R. Morrison & P. L. Strick), pp. 281–293. New York: Academic Press.

Sterling, P. 1983 Microcircuitry of the cat retina. *Ann. Rev. Neurosci.* **6**, 149–185.

Sterling, P., Freed, M. & Smith, R. G. 1988 Architecture to rod and cone circuits to the on-beta ganglion cell. *J. Neurosci.* **8**, 623–642.

Stevens, J. K., Davis, T. L., Friedman, N. & Sterling, P. 1980 A systematic approach to reconstructing microcircuitry by electron microscopy of serial sections. *Brain Res. Rev.* **2**, 265–293.

Wässle, H., Levick, W. R. & Cleland, B. G. 1975 The distribution of the alpha type of ganglion cells in the cat's retina. *J. Comp. Neurol.* **159**, 419–438.

Wässle, H., Peichl, L. & Boycott, B. B. 1978 Topography of horizontal cells in the retina of the domestic cat. *Proc. R. Soc. Lond.* **203**, 269–291.

Wässle, H., Boycott, B. B. & Illing, R. B. 1981*a* Morphology and mosaic of on- and off-beta cells in the cat retina and some functional considerations. *Proc. R. Soc. Lond.* B **212**, 177–195.

Wässle, H., Peichl, L. & Boycott, B. B. 1981*b* Morphology and topography of on- and off-alpha cells in the cat retina. *Proc. R. Soc. Lond.* B **212**, 157–175.

(*Submitted by Professor B. B. Boycott, F.R.S.; received 22 March 1990; revised 2 August 1990*)

PHILOSOPHICAL TRANSACTIONS OF THE ROYAL SOCIETY B BIOLOGICAL SCIENCES

(*a*)

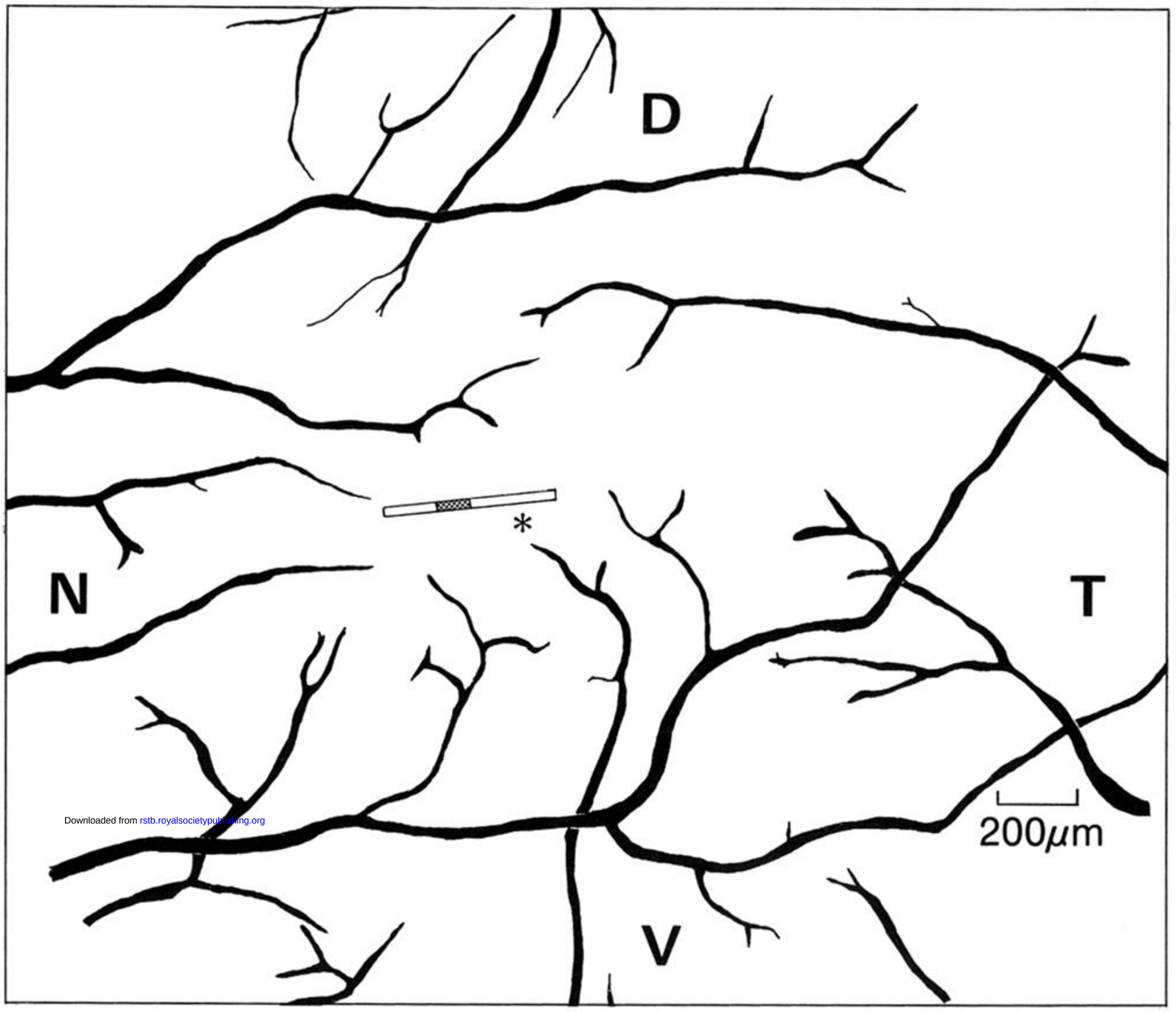

(*b*)

Figure 1. (*a*) Drawing of the area centralis in retinal wholemount. Converging dark lines represent blood vessels on the retinal surface which are seen to avoid the area centralis. Rectangle shows location and extent of tissue used for thin sections; hatched area shows region photographed in the electron microscope. The star marks centre of area centralis as estimated from the peak of ganglion cell density in the wholemount. N, nasal; T, temporal; D, dorsal; V, ventral. (*b*) Electron micrograph (low magnification) of section 274. Brackets show the region analysed. Neurons in the ganglion cell layer (GCL) form a continuous tier at this location, and blood vessels are absent. OS, outer segments; ONL, outer nuclear layer; OPL, outer plexiform layer; INL, inner nuclear layer; IPL, inner plexiform layer.

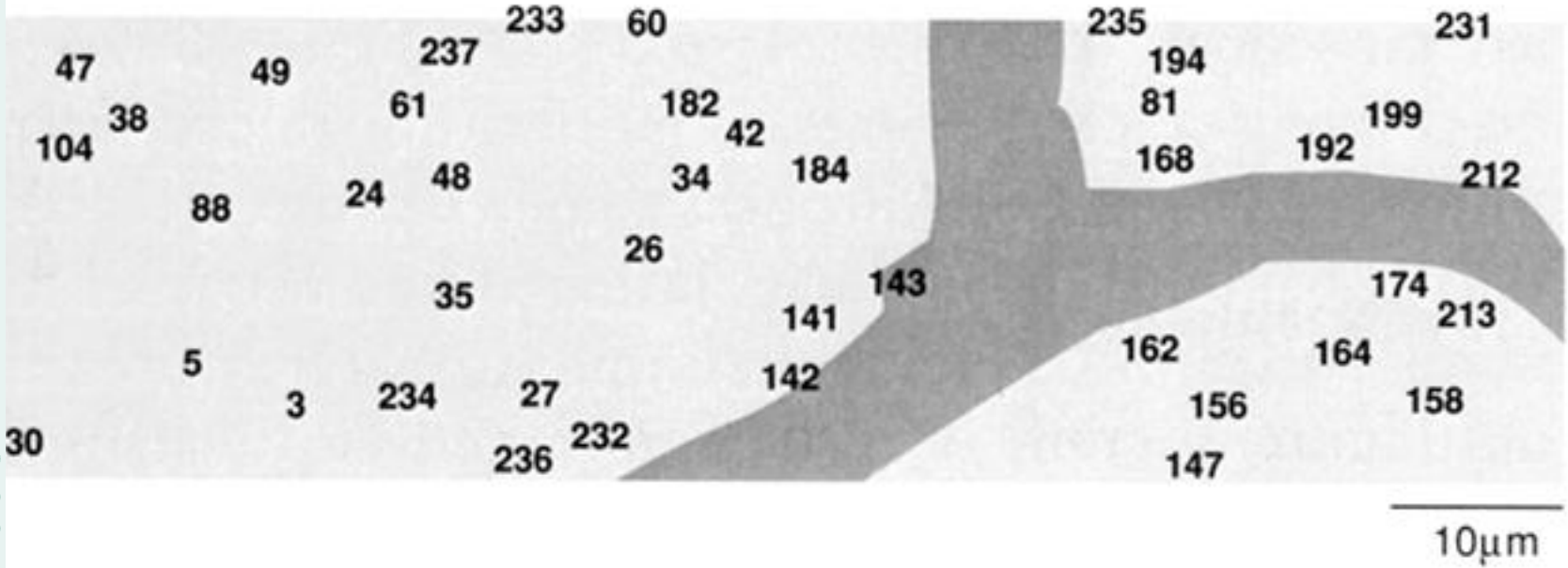

igure 2. Location in tangential plane of all 42 cone bipolar xons that arborize in sublamina *b*. Distribution density, 9250 per square millimetre; nearest neighbour distance, .9 ± 4.4 μm. Shaded area indicates blood vessel at the unction of sublaminae *a* and *b*.

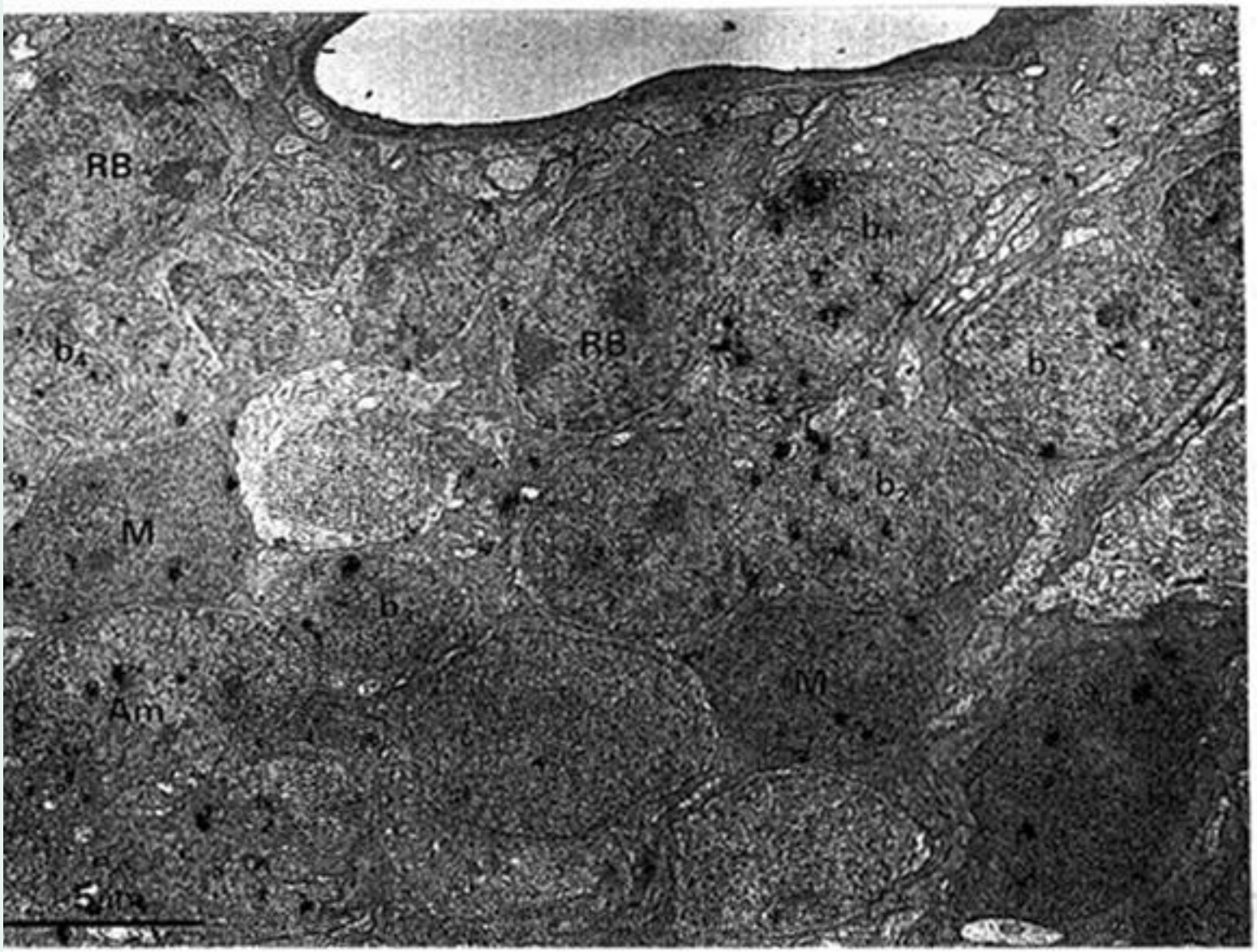

igure 4. Electron micrograph of the inner nuclear layer NL) (vertical view). Somas of different cone bipolar ategories are roughly similar in size and cytological ppearance, but occupy different levels in the INL (see figure). RB, rod bipolar; M, Muller cell; Am, amacrine cell.

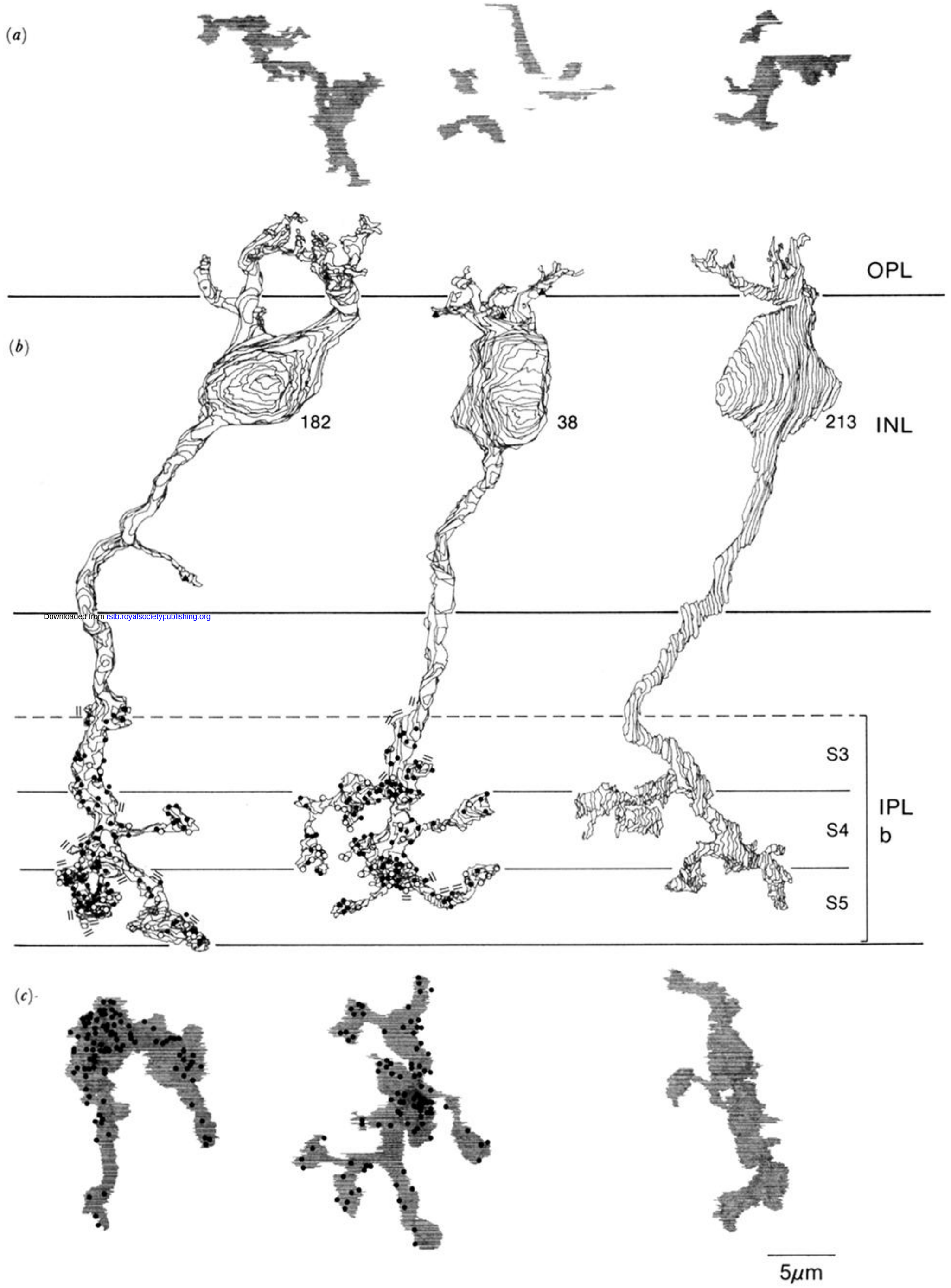

Figure 5. (*a*) Dendritic arbor of each cell in tangential view. (*b*) Reconstructions in vertical view of three b_1 bipolar neurons. Numbers next to soma are for identification. Dots, sites of chemical synaptic output; open circles, sites of chemical synaptic input; triangles, chemical synaptic contacts presumed to be from interplexiform cell; double bars, sites of gap junction with AII amacrine cells; single bars, sites of gap junction with cone bipolar cell. (*c*) Axonal arbor of each cell in tangential view. Dots mark sites of chemical synaptic output.

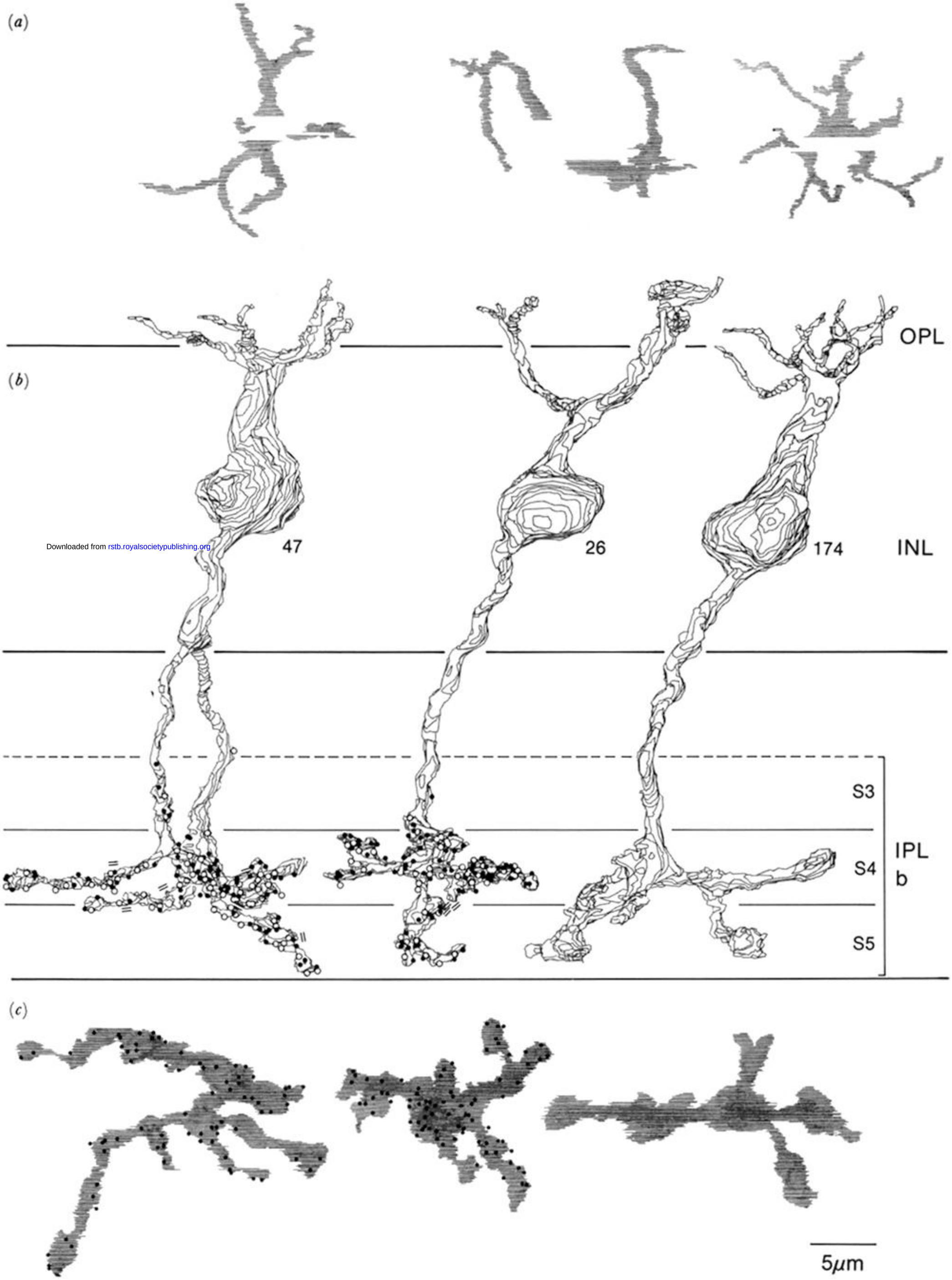

Figure 6. (*a*) Dendritic arbor of each cell in tangential view. (*b*) Reconstructions in vertical view of three b_2 bipolar neurons. (*c*) Axonal arbor of each cell in tangential view. Symbols as for figure 5.

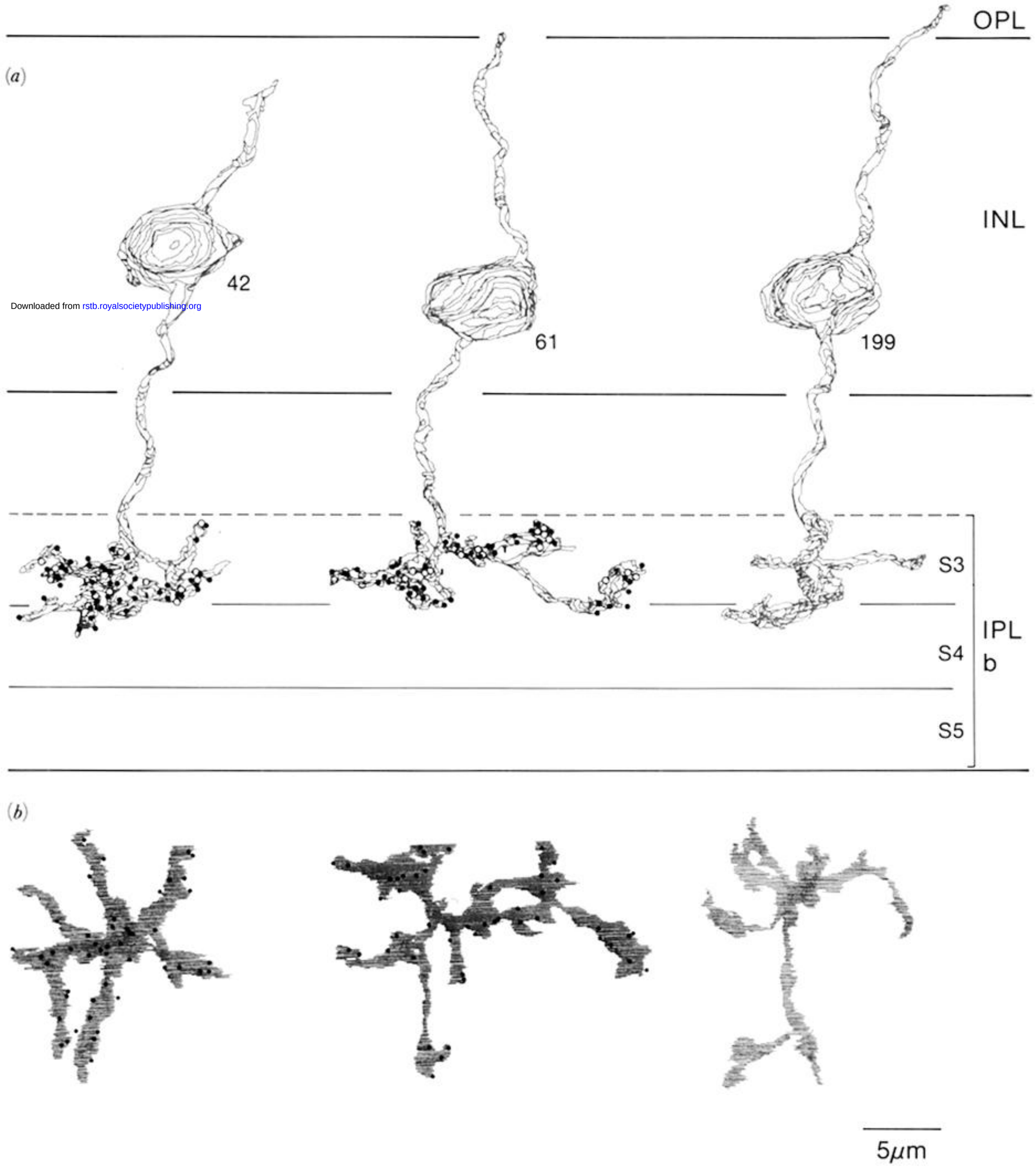

igure 7. (*a*) Reconstructions in vertical view of three b_3 bipolar neurons. (*b*) Axonal arbor of each cell in tangential view. Symbols as for figure 5.

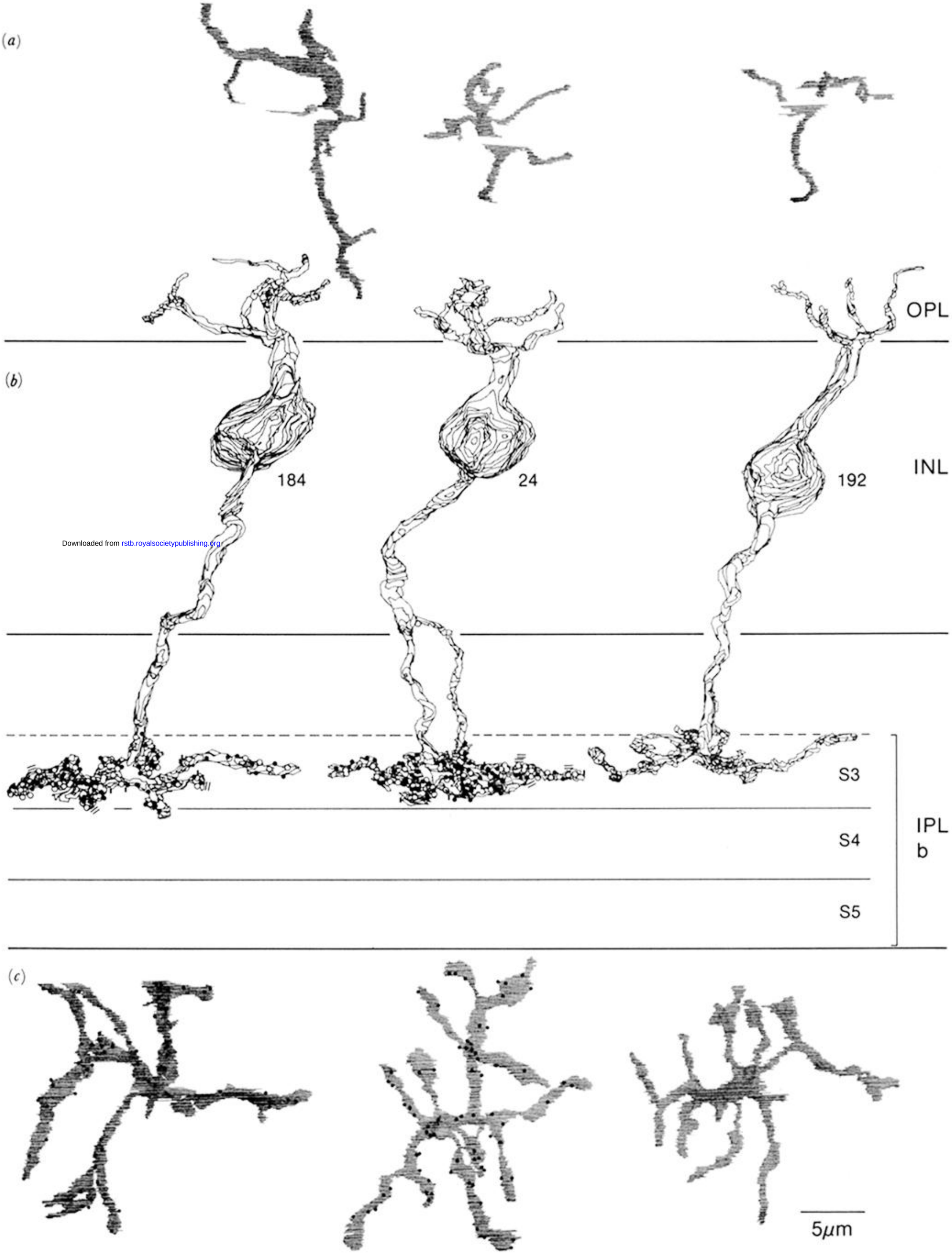

PHILOSOPHICAL TRANSACTIONS OF THE ROYAL SOCIETY B BIOLOGICAL SCIENCES

igure 8. (*a*) Dendritic arbor of each cell in tangential view. (*b*) Reconstructions in vertical view of three b_4 bipolar neurons. (*c*) Axonal arbor of each cell in tangential view. Symbols as for figure 5.

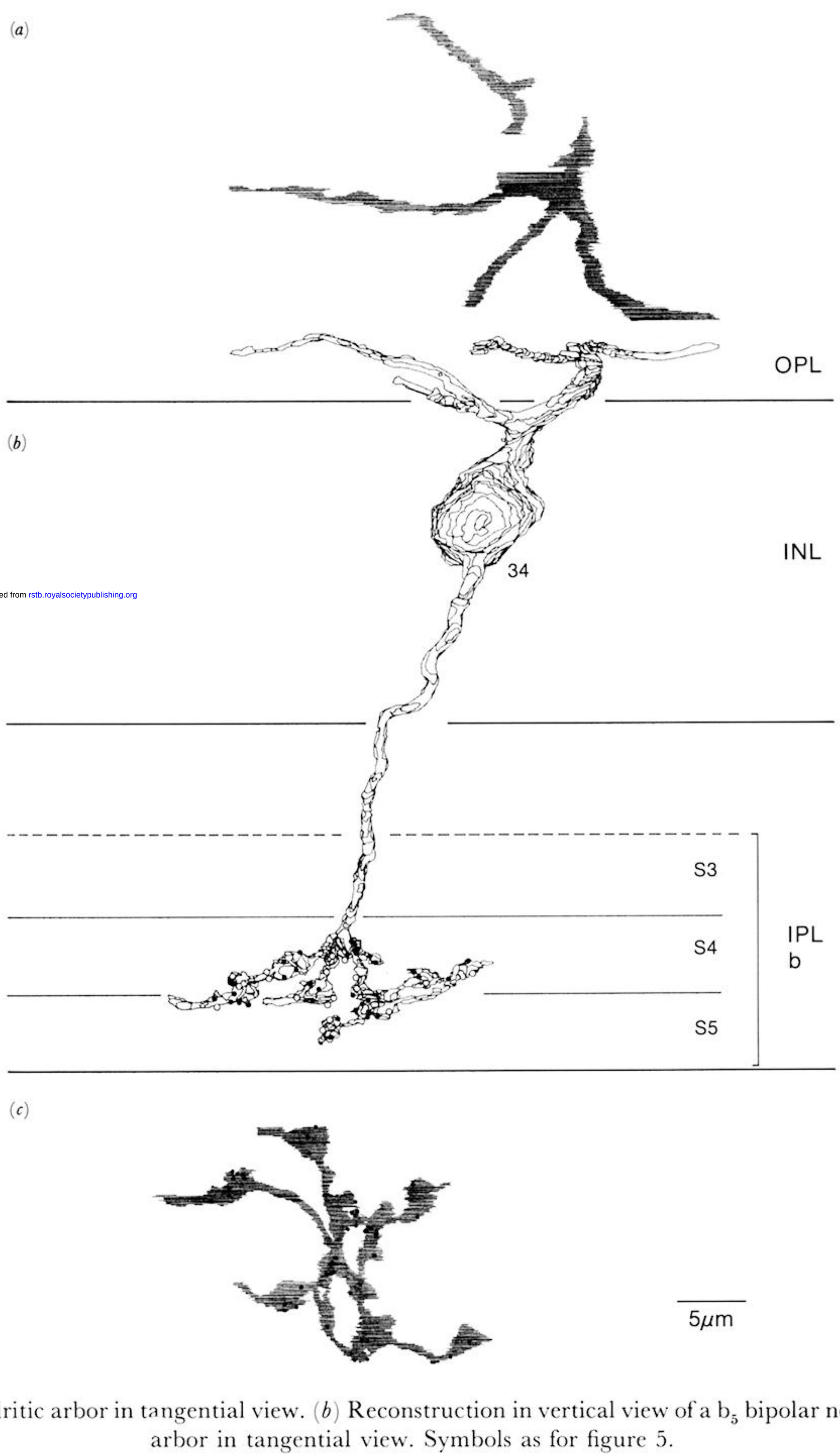

gure 9. (*a*) Dendritic arbor in tangential view. (*b*) Reconstruction in vertical view of a b_5 bipolar neuron. (*c*) Axonal arbor in tangential view. Symbols as for figure 5.

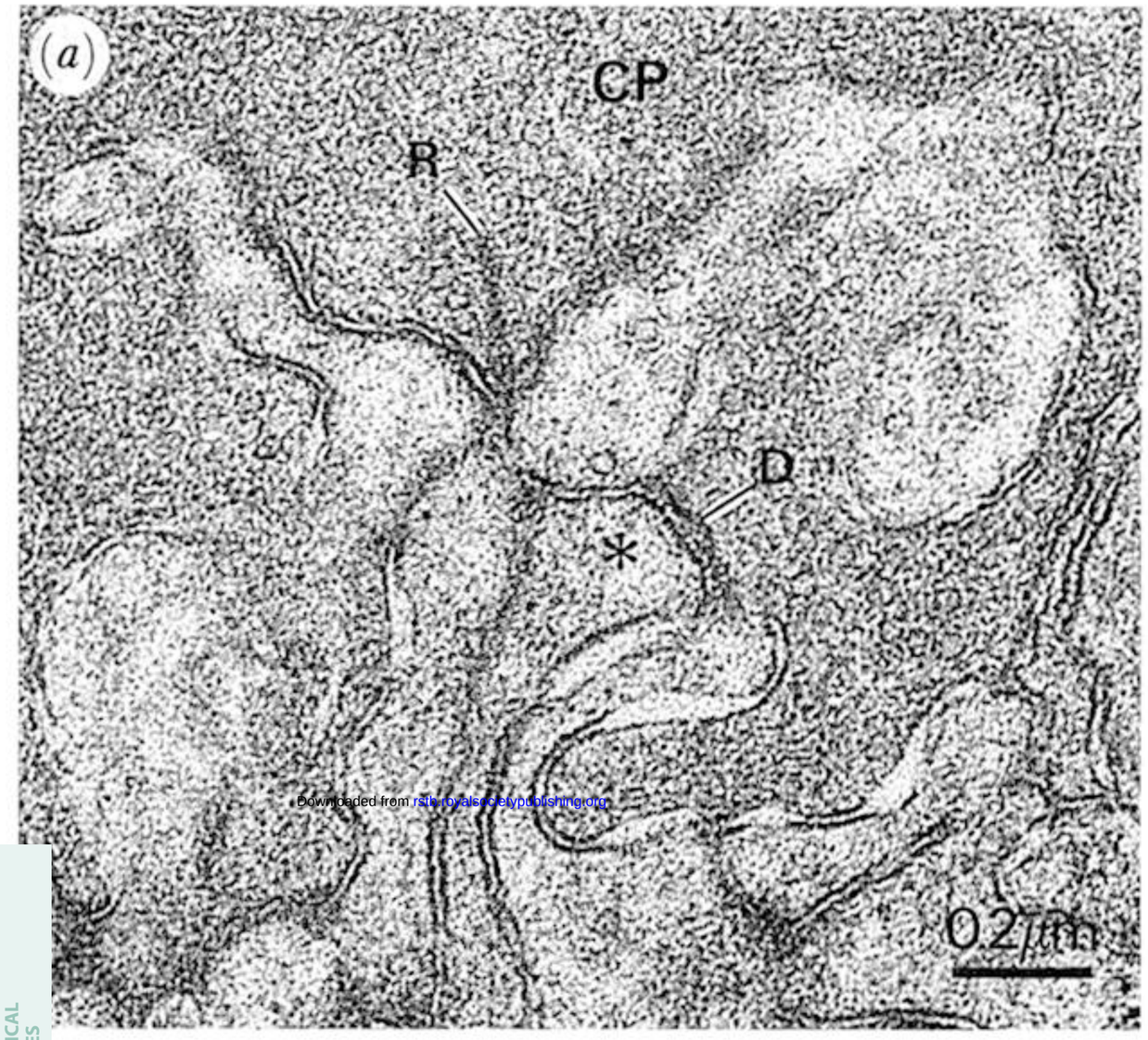

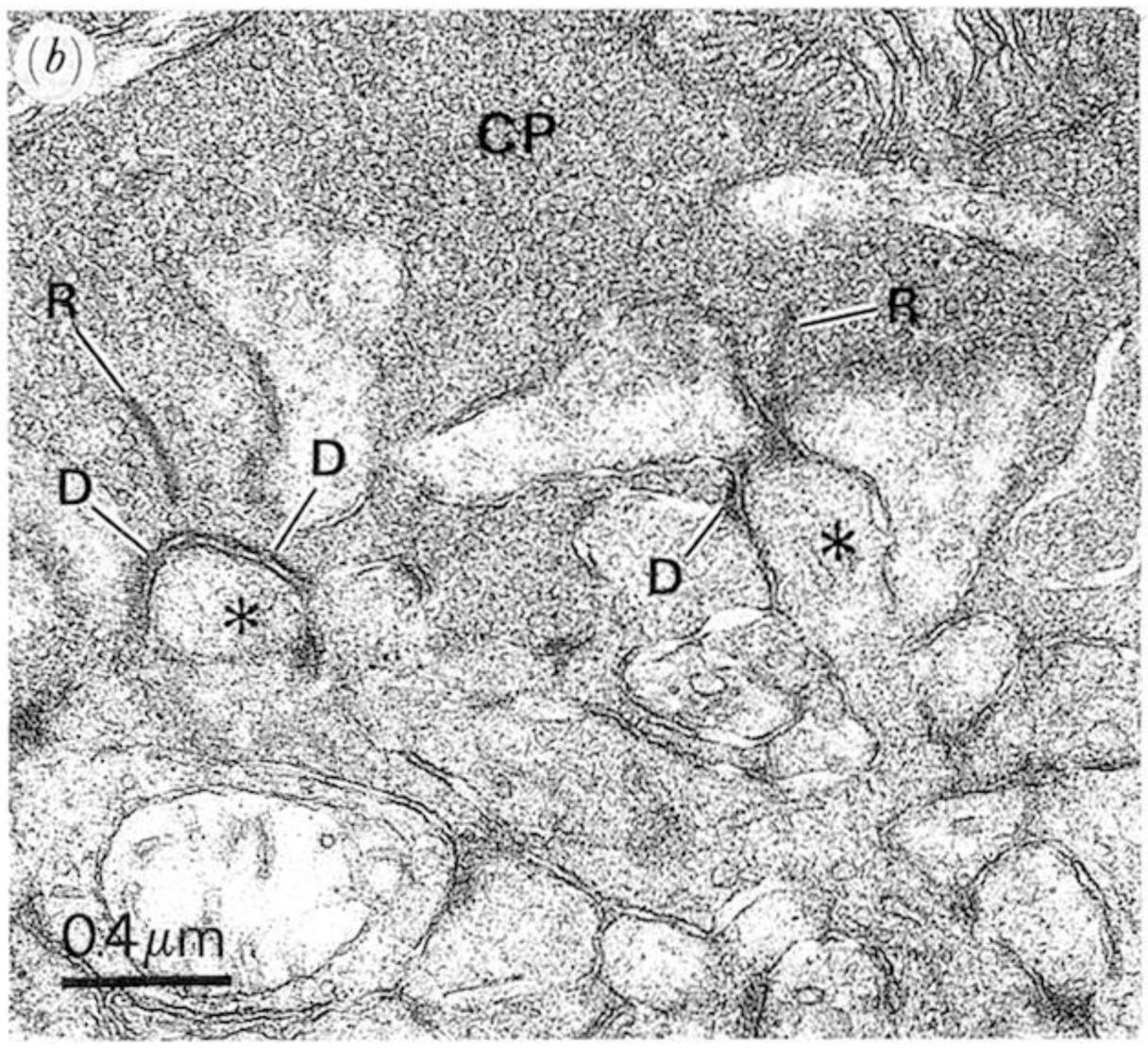

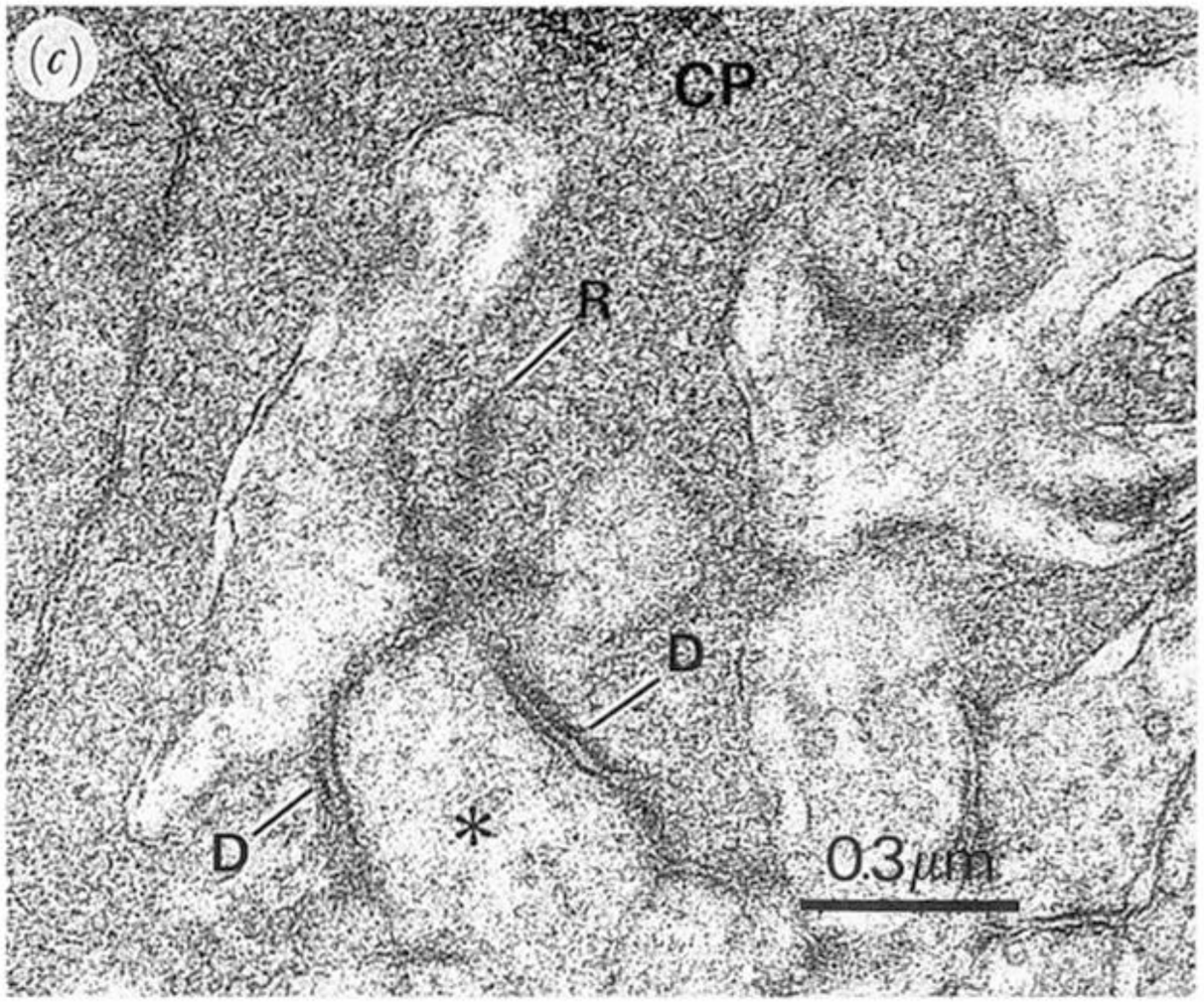

Figure 10. Electron micrographs of synaptic contacts between cone pedicle and bipolar dendrites. (*a*) b_1 dendrite (*) pushes part way into the pedicle ('semi-invaginating') and is post-synaptic to cone at site (D) some distance from the ribbon. Another dendrite, unidentified as to type, terminates just beneath the ribbon ('fully invaginating'). R, ribbon; CP, cone pedicle. (*b*) Two thorns (*) from a single b_2 dendrite invaginate a cone pedicle fully and form post-synaptic density just beneath the synaptic ribbon. (*c*) b_4 dendrite fully invaginates the cone pedicle to form post-synaptic density just beneath the ribbon and also a density (D) at some distance from the ribbon.

PHILOSOPHICAL TRANSACTIONS OF THE ROYAL SOCIETY B BIOLOGICAL SCIENCES

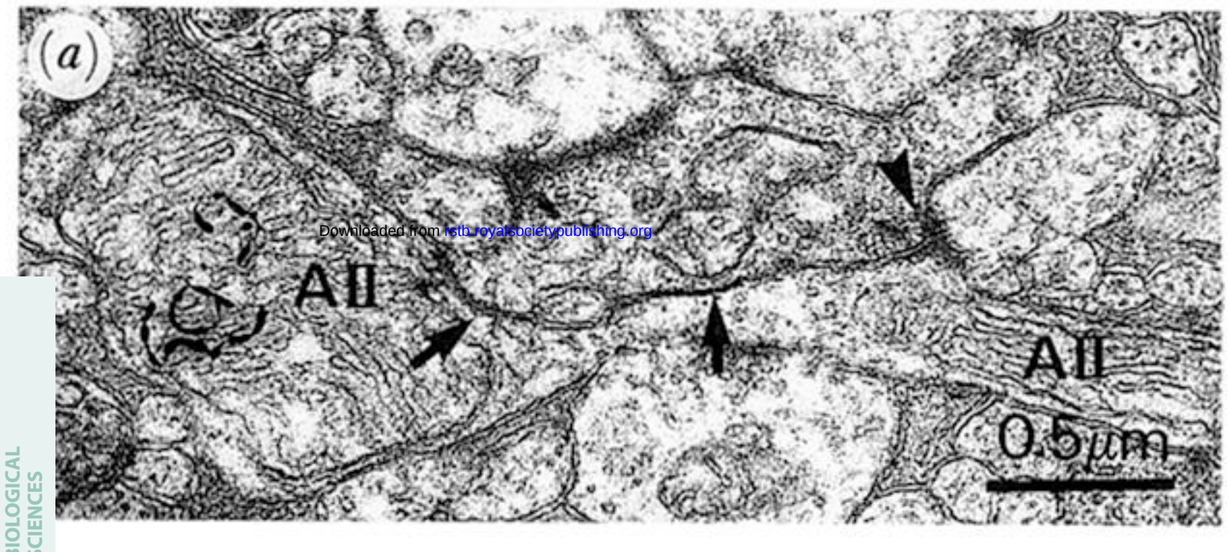

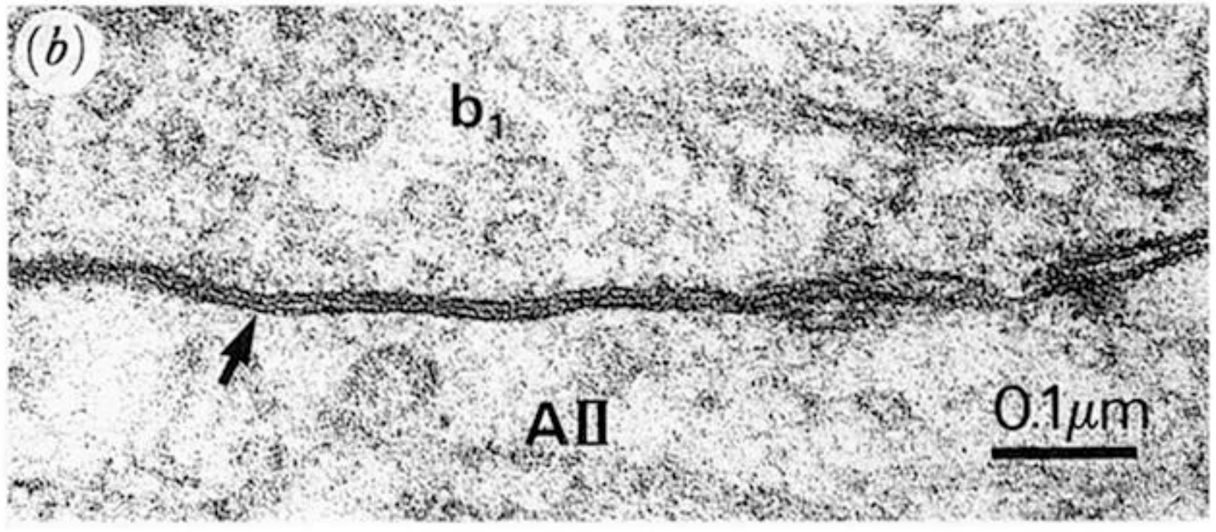

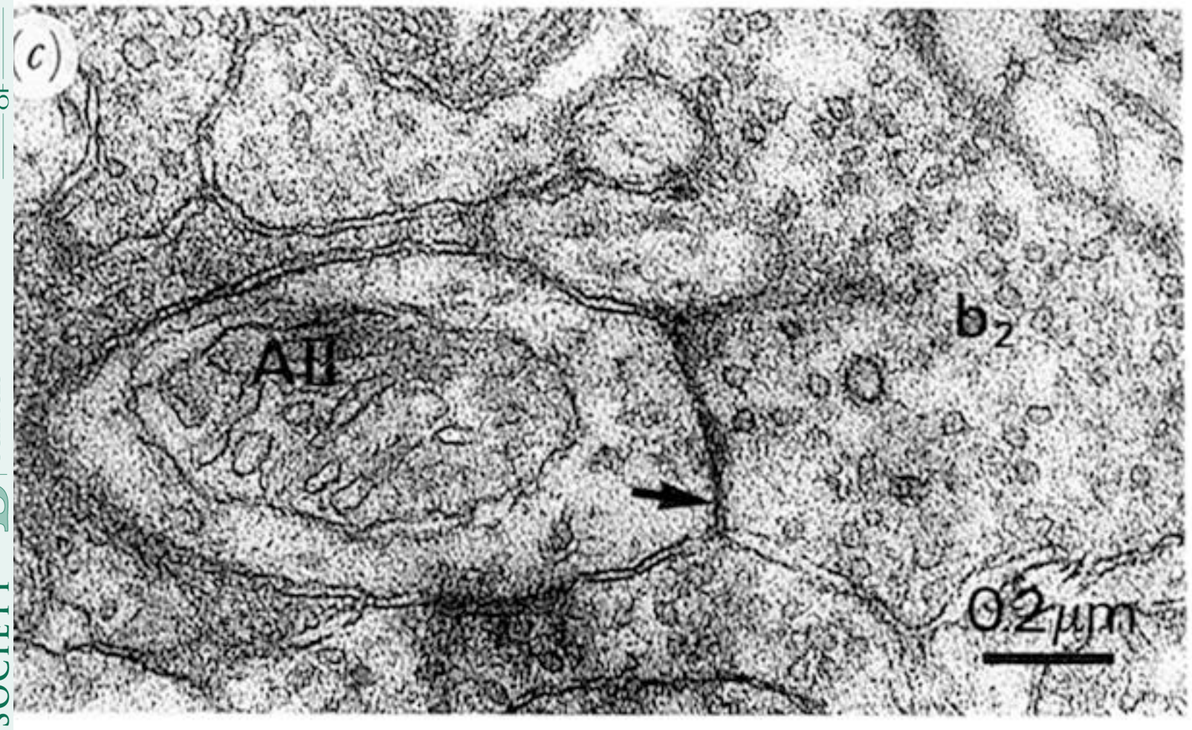

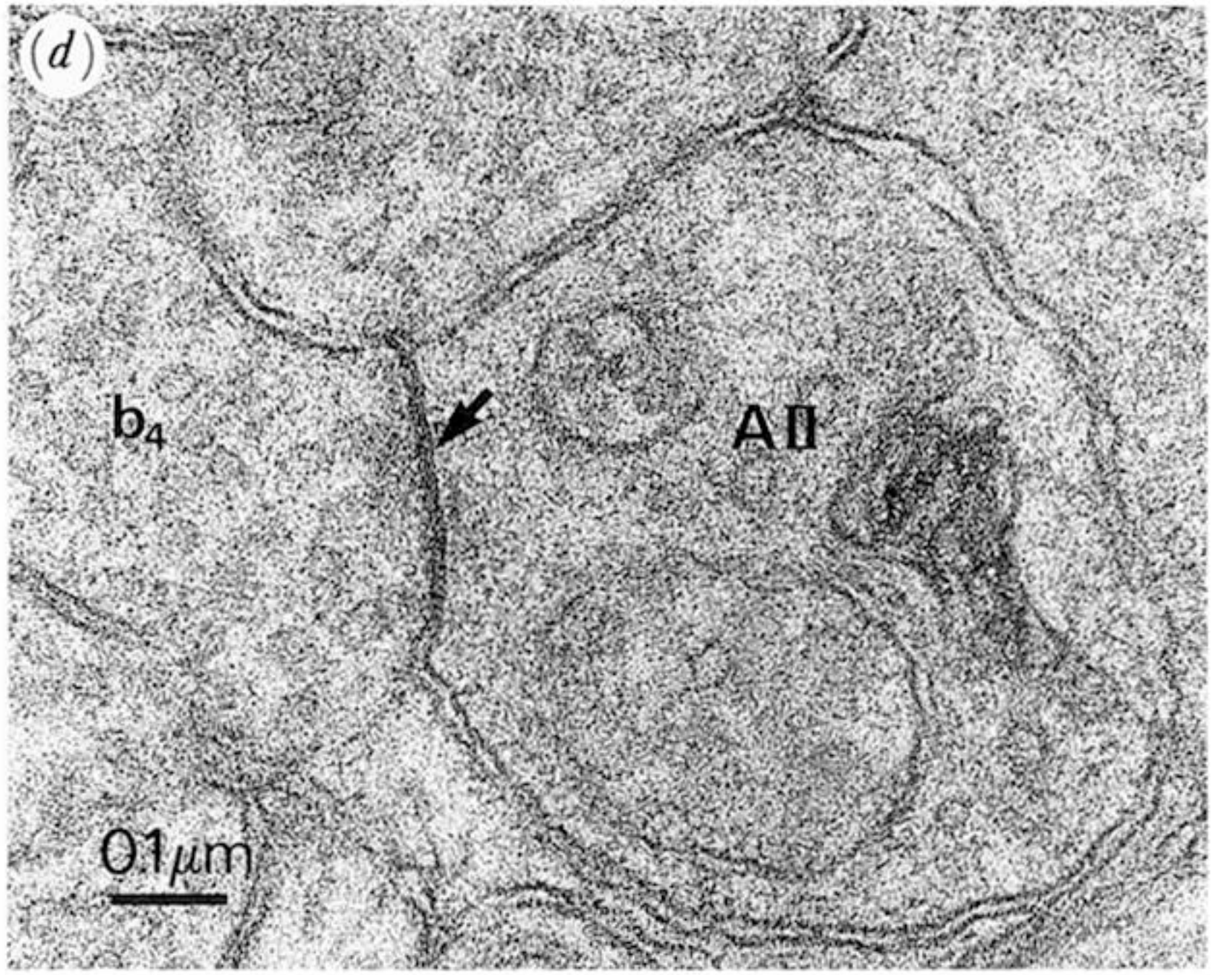

Figure 11. Gap junctions between cone bipolar axons and AII amacrine processes. (*a*) b_1 axon (note ribbon) forms two gap junctions (arrows) with AII. b_1 axon also provides a chemical synapse (arrowhead) to the AII cell. This connection was exceptional (because most bipolar chemical synapses to the AII derived from the rod bipolar) and only two other examples of b_1–AII chemical synapse were observed. (*b*) b_1–AII gap junctions at higher magnification. (*c*) b_2–AII gap junction. (*d*) b_4–AII gap junction.

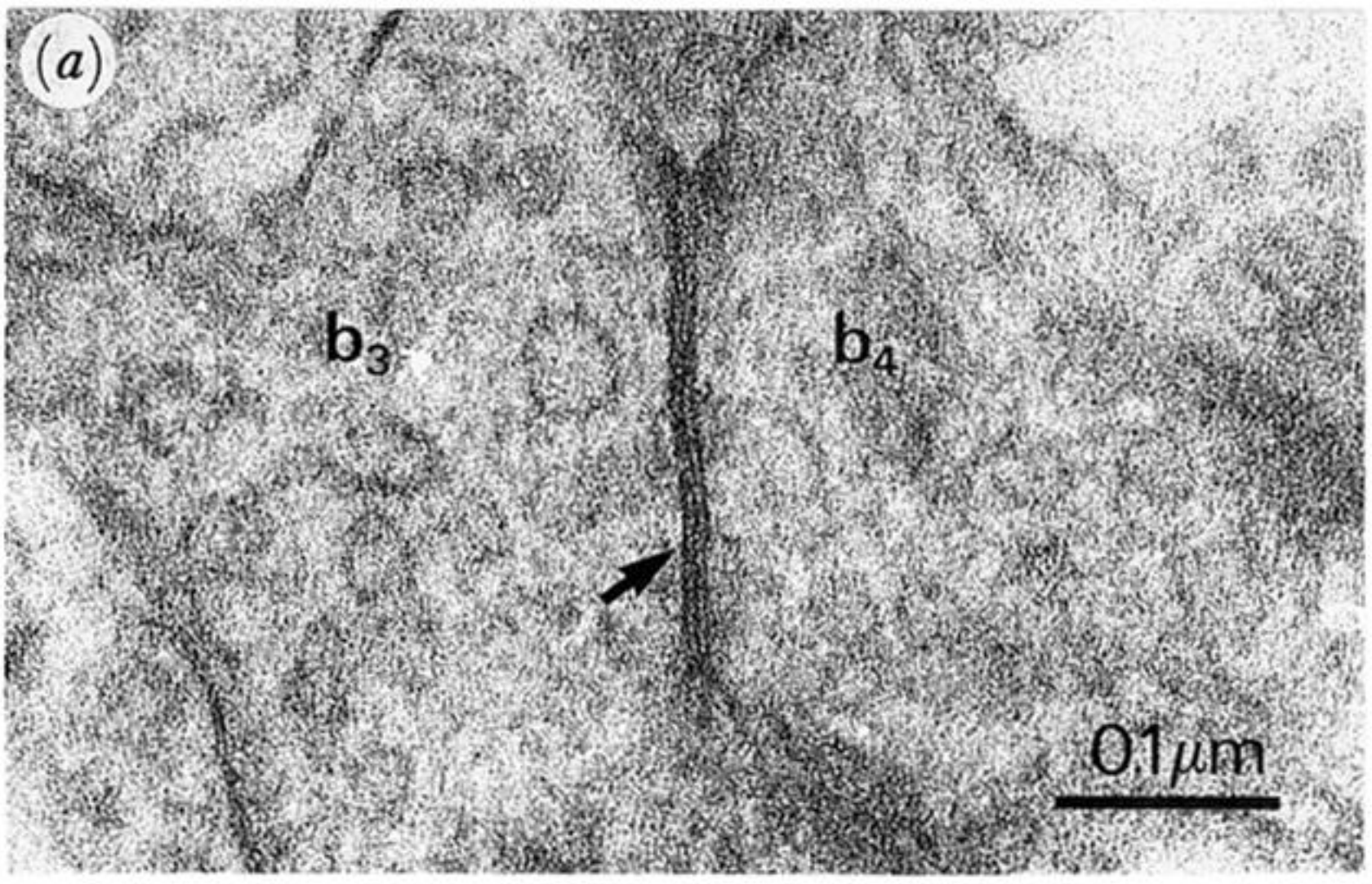

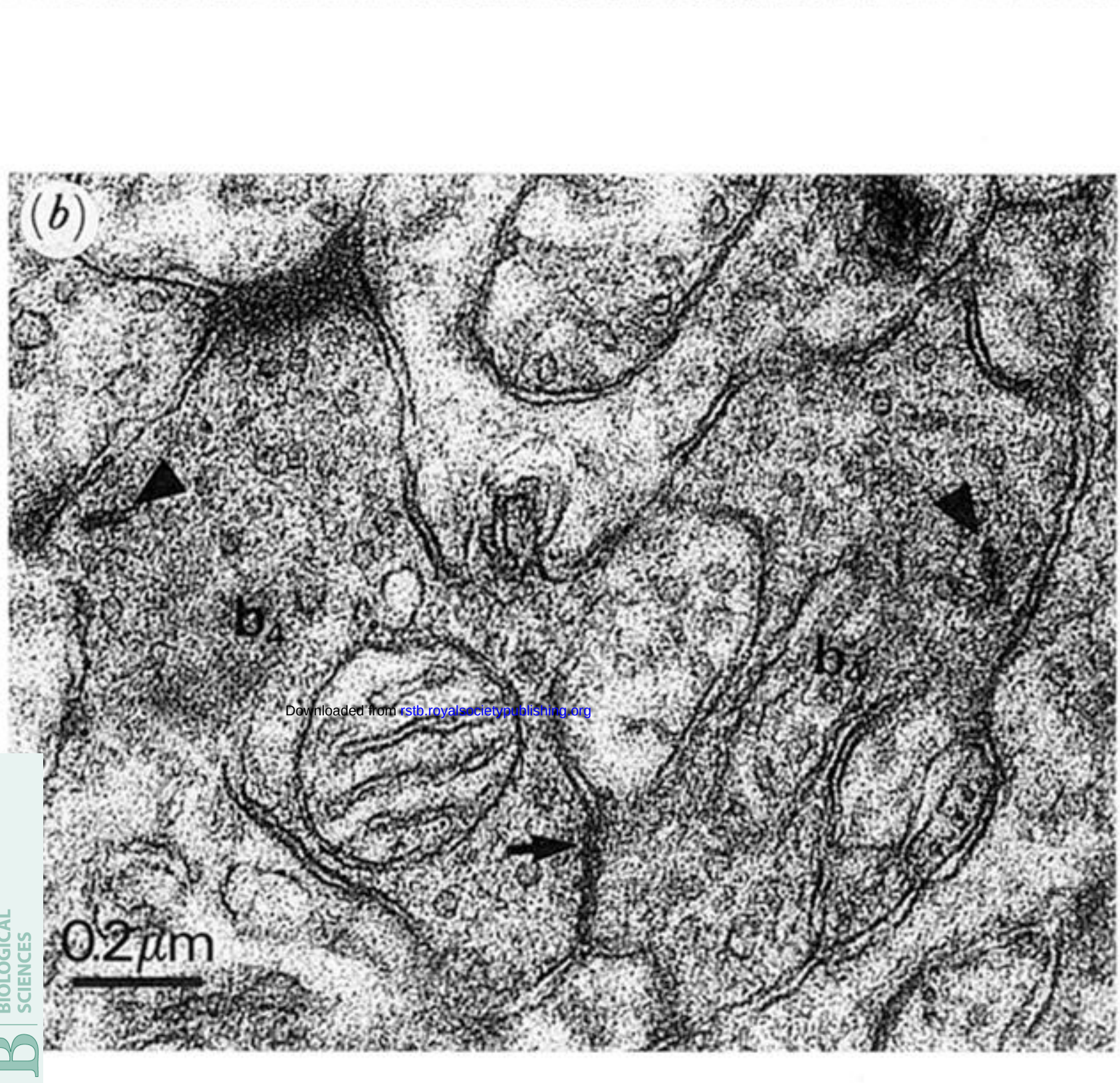

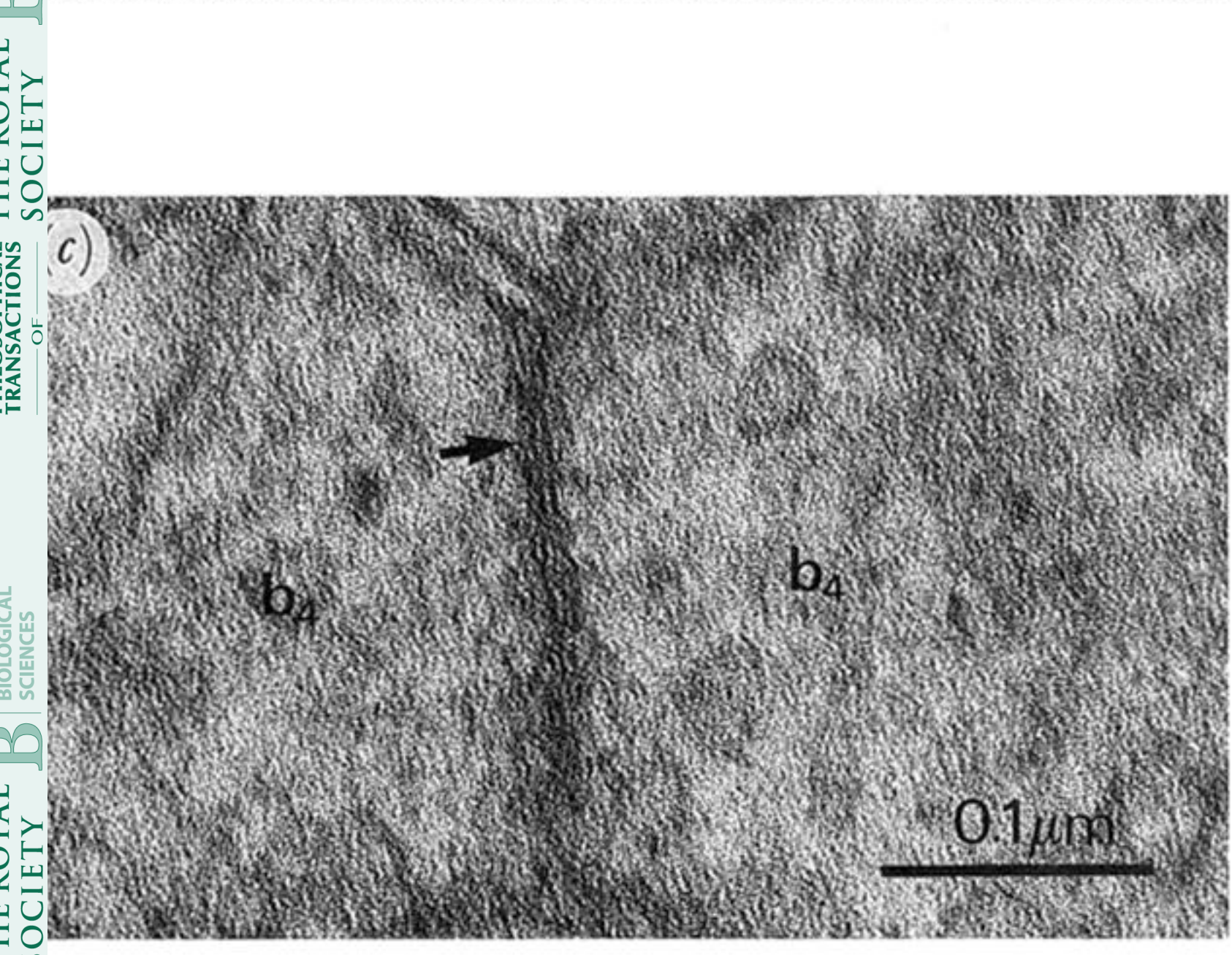

PHILOSOPHICAL TRANSACTIONS OF THE ROYAL SOCIETY B BIOLOGICAL SCIENCES

igure 12. Gap junctions between bipolar axons. (*a*) Gap nction between b_3 and b_4 processes. (*b*) Two b_4 processes rrowheads mark synaptic ribbons) form gap junction rrow). (*c*) Higher magnification of same junction in the djacent section.

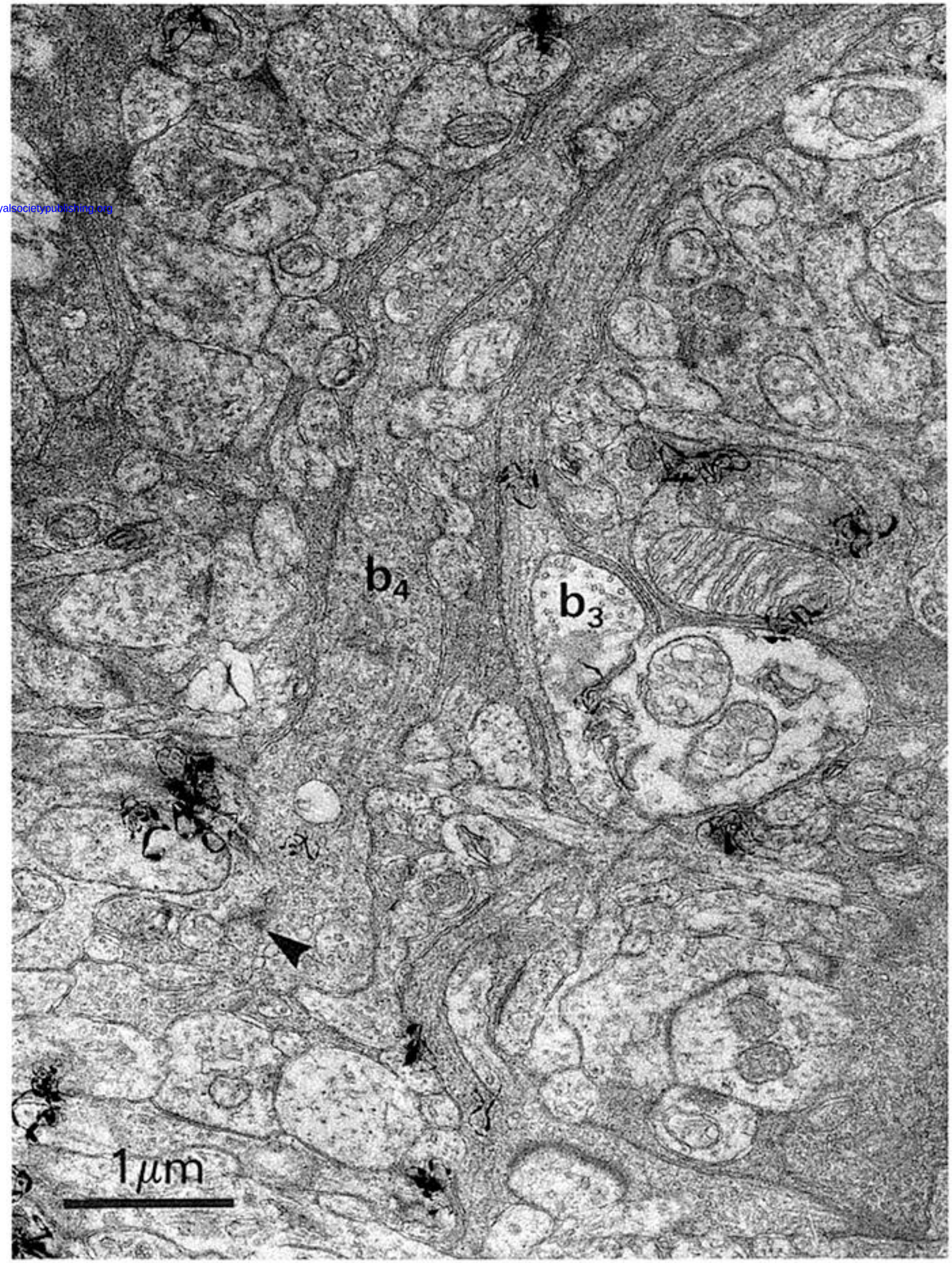

igure 13. Electron micrograph of adjacent cone bipolar axons. The b_3 axon (cell 199; see figure 7) is thin; the b_4 axon (cell 192; see figure 8) is thicker. Arrowhead points to synaptic ribbon in b_4 axon.